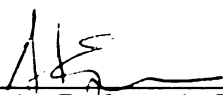This is to certify that the
dissertation entitled

A Novel Technique for Steam Turbine Exhaust-Pressure Limit
Control Using Dynamic Pressure Transducers

presented by

Muhammad Saqib Riaz

has been accepted towards fulfillment
of the requirements for the

_____Ph.D._____ degree in _____Mechanical Engineering_____

_____
Major Professor's Signature

_____12|08|05_____

Date

**PLACE IN RETURN BOX** to remove this checkout from your record.
**TO AVOID FINES** return on or before date due.
**MAY BE RECALLED** with earlier due date if requested.

| DATE DUE | DATE DUE | DATE DUE |
|----------|----------|----------|
|          |          |          |
|          |          |          |
|          |          |          |
|          |          |          |
|          |          |          |
|          |          |          |
|          |          |          |
|          |          |          |
|          |          |          |
|          |          |          |

A NOVEL TECHNIQUE FOR STEAM TURBINE EXHAUST-PRESSURE LIMIT
CONTROL USING DYNAMIC PRESSURE TRANSDUCERS

By

Muhammad Saqib Riaz

A DISSERTATION

Submitted to
Michigan State University
in partial fulfillment of the requirements
for the degree of

DOCTOR OF PHILOSOPHY

Department of Mechanical Engineering

2005

.

# ABSTRACT

A NOVEL TECHNIQUE FOR STEAM TURBINE EXHAUST-PRESSURE LIMIT
CONTROL USING DYNAMIC PRESSURE TRANSDUCERS

By

Muhammad Saqib Riaz

A novel approach is presented to increase the operational flexibility of steam turbines. Pressure at the exhaust of the last stage of a condensing steam turbine is one of the most important parameters that limit the operation of a steam turbine - especially on days with hot ambient temperature. On these days when the power demand is at its peak, the power plant may be forced to reduce power production due to insufficient condenser cooling capability in order to maintain exhaust-pressure within specified limits.

The main concern in operating at these off-design high exhaust-pressures is that it can result in flow separation which can lead to aerodynamics instabilities and thus to blade vibration and failure due to high cycle fatigue. Current exhaust-pressure limits are generally established based on experience and are conservative in order to protect the blade from catastrophic failure. This research proposes a new method to place dynamic pressure transducers around the perimeter of the last stage blades to measure pressure variations caused by vibrating blades. This approach will enable real-time monitoring of the pressure signal, enabling real time detection of blade vibration, thereby allowing operation at increased exhaust-pressures without risk to the last stage blade, ultimately enabling the power plants to produce more power during times of peak demand.

A deep insight into the phenomenon of aerodynamics instabilities in steam turbines was obtained and parameters that influence stability were identified. Finite element analysis was used to predict the modal and structural response of a full row of blades. CFD analysis was performed to predict the impact of higher exhaust-pressures on the steam flow at the exit of the last stage blade. Two distinct experiments were conducted on a subscale low-pressure steam turbine. In both tests, different sets of blades, nozzles and steam path hardware were used. The first test was conducted to identify the appropriate pressure transducers and understand the proposed technique. In the second test, the transducers were applied at wide range of turbine operating conditions by changing steam mass flow, exhaust-pressure and turbine speed. The dynamic pressure transducers responded accurately in all operating conditions. FE analysis predictions were validated using test results. Dynamic pressure transducer response was compared with strain gauge response and an excellent agreement was observed between two sets of data. The transducers were clearly able to identify the lower as well as higher order modes of vibrations. Details are provided to define allowable dynamic pressure amplitudes based on the material capabilities of the blades, thereby allowing the blades to operate to their maximum capabilities.

Successful application of this technique will allow a wider range of operating conditions and hence a more reliable and profitable steam turbine. This unique technology will have a direct impact on the power production in high demand seasons and can result in increased profitability for the turbine operators.

To my parents' innumerable sacrifices and untiring support throughout my life

# ACKNOWLEDGEMENT

# TABLE OF CONTENTS

# CHAPTER 4. DYNAMIC PRESSURE TRANSDUCERS

# CHAPTER 5. EXPERIMENTAL DESIGN AND SETUP

# CHAPTER 6. ANALYTICAL PREDICTIONS

# CHAPTER 7. EXPERIMENTAL RESULTS AND COMPARISON

# CHAPTER 8.

# LIST OF TABLES

# LIST OF FIGURES

# NOMENCLATURE

$C$        Chord (length) of the airfoil

$C_L, C_D, C_M$   Lift, drag and moment coefficient

$F_y'$      Vertical aerodynamic force/ unit span

$F_\theta'$      Aerodynamic moment/ unit span

$F_L, F_D, F_M$   Lift, drag and moment force

$F.S.$         Factor of safety

$K_y, K_\theta$       Spring stiffness constant for linear and torsional spring

R        Blade tip radius

Re       Reynolds number

T        Time

U        Free stream velocity

$X_0$       Distance between the leading edge and elastic axis

$a_u$       Circumferential component of the blade vibration amplitude

b        Circumferential distance between two sensors

$J_\theta$       Mass moment of inertia

$m$        Mass

n        Rotor rotational speed

u        Blade circumferential velocity

$y$        Vertical displacement

z        Blade number

$z_b$    Sensor distance as multiple of blade pitch

# Greek

$\Delta h_{rot}$    Change in static enthalpy of the rotor

$\Delta h_{stage}$    Change in static enthalpy of the stage

$\Delta t$    Passing time between two sensors

$\Delta y$    Difference of blade tip vibration deflections

$\Delta y_{max}$    Maximum deflection difference of the blade vibration

$\Omega$    Rotor speed

$\alpha$    Angle of attack between airfoil axis and flow

$\zeta_y, \zeta_\theta$    Damping Factors

$\theta$    Angle of twist

$\omega_y$    Natural frequency of the body

$\omega$    Excitation frequency

$\rho$    Density of the airfoil material

$\upsilon$    Kinematic viscosity.

$\sigma_{SS}$    Steady State Stresses

$\sigma_{vib}$    Vibratory or Alternating Stresses

# CHAPTER 1

# INTRODUCTION

Turbines are used to generate power by converting thermal energy into mechanical energy. Steam at high temperature and pressure is passed through a series of stationary and moving sets of blades converting thermal energy into mechanical energy. A generator is then used to produce electrical power from the mechanical energy. Steam turbines have been vital part in both large and small power plants and industrial steam systems for more than a hundred years. There are two general categories of steam turbines: Condensing and Non-condensing. Condensing turbines exhaust steam at less than atmospheric pressure to a condenser where a vacuum is maintained. In the non-condensing turbine, the exhaust steam is used for industrial process.

Pressure at the exhaust of the last stage of the steam turbine blades is one of the most important parameters that limit the operation of a steam turbine. Currently there is a great interest in industry to operate turbines at wider operating range, particularly at high exhaust-pressures. The purpose of this study is to understand the problems associated with operation at higher exhaust-pressures and to provide a method to increase the operational flexibility of steam turbines with respect to variations in ambient temperature and/or condenser cooling capability.

## 1.1    Problem Definition

As mentioned before, steam leaving the turbine enters into the condenser at pressure lower than atmospheric pressure. For condensing steam turbines, the condenser cooling capability can be limiting due to condenser size, cooling water inlet temperature, or more importantly, inlet air temperature for air-cooled condensers. This results in inability to achieve maximum steam expansion in the turbine, and or the need to reduce the heat load on the condenser to maintain vacuum within prescribed limits. Reducing heat load can only be accomplished by reducing power. It is particularly limiting on hot days for air condensers or for periods with insufficient cooling water capability for water-cooled condensers. However, these days or periods of limited cooling capability are often the times when electric power demand is greatest and selling prices are highest. Limited cooling capacity results in a higher exhaust-pressure that forces the plant operators to reduce output so that exhaust-pressure returns to acceptable levels. Typically the allowed exhaust-pressure ranges from 3 kPa to 50 kPa (1 in HgA to 15 in HgA) depending on the last stage blade capability. Operation at higher than recommended exhaust-pressures can lead to off design aerodynamic operating conditions. At these conditions, the incidence angle changes and may cause flow separation resulting in onset of aerodynamics instabilities such as buffeting, un-stalled flutter and stall flutter; causing potentially negative impact on the turbine blades. Flow separation can occur resulting in blade excitation, high vibratory response and potential for a blade failure due to high cycle fatigue. The last stage blades are the most vulnerable hardware in this case. A solution to the problem of aerodynamically induced non-synchronous vibrations can be achieved

2

through a reliable process that can provide instantaneous vibratory information of these blades in a non-intrusive and highly reliable manner.

For condensers with limited cooling capacity, the alternatives to reduce exhaust-pressure to design point is either to build a bigger condenser or to reduce mass flow rate (heat input to the condenser) through the turbine thereby reducing the power output from the turbine. Figure 1.1 shows lines of constant mass flow rate plotted versus exit velocity and exhaust-pressure. For a constant exit velocity, the exhaust-pressure increases with increasing mass flow rates. In order to achieve maximum output, the turbine operators must operate at maximum available flow rate, and minimum exhaust pressure. However in high ambient temperature conditions, exhaust pressure will increase. The only remedy the turbine operator has to limit exhaust-pressure below the allowable is to reduce mass flow rate, and thus reduce the power output.

Conventionally, the control on the exhaust-pressure is provided by a set of data points that define an alarm and trip limit. When the Alarm limit is reached on exhaust-pressure a signal is sent to the operator and necessary measures should be taken to bring the exhaust-pressure down. At Trip limit the turbine automatically shuts down. Figure 1.2 shows the control system of steam turbine. These limits differ from manufacturer to manufacturer and the allowable exhaust-pressure limits are also a function of the capability of the last stage blade. For condensing turbines, the recommended exhaust pressure is established through the design of several last stages and the capability of the condenser to accept the exhaust heat energy. Current exhaust-pressure limits are

generally established based on experience and are very conservative. There is a need to develop a robust method to measure the vibrations of the last stage blades caused by these aerodynamics instabilities to provide increased exhaust-pressure limits, enabling the power plant to produce more power during times of peak demand.
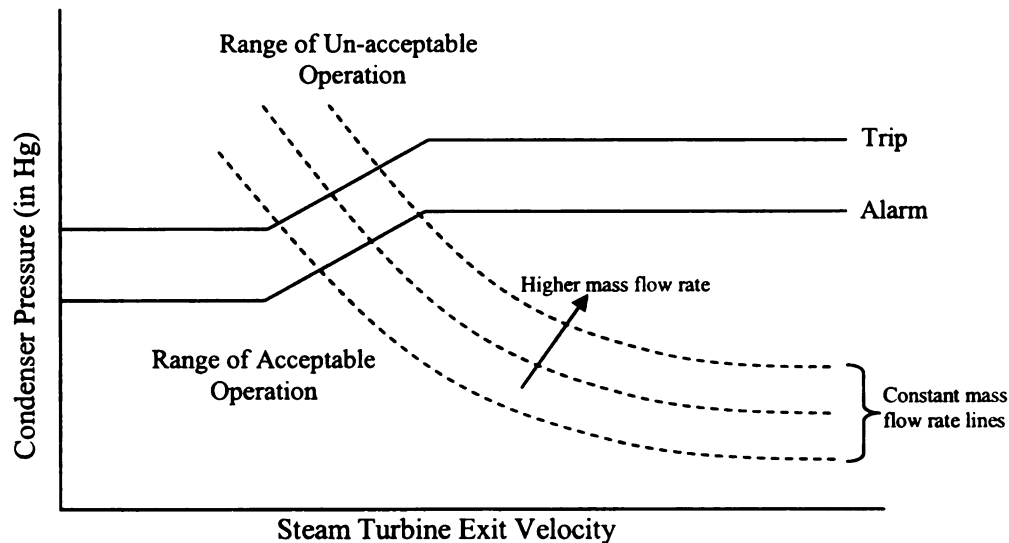


Figure 1.1 Conventional alarm and trip limits for a steam turbine

## 1.2    Proposed Solution

The present control system to protect against aerodynamics instabilities provides set points for alarm and trip based solely upon static pressure level. Because the limits are based solely upon static pressure, they tend to be conservative. It is proposed to use dynamic pressure sensors at the perimeter of the last stage blade to detect the varying pressure amplitudes present in the steam medium due to blade vibration. Synchronous and non-synchronous vibrations can be differentiated with the knowledge of blade natural

4

frequencies that are excited only by the engine orders. Blade natural frequencies are obtained from finite element analysis and blade vibration tests.
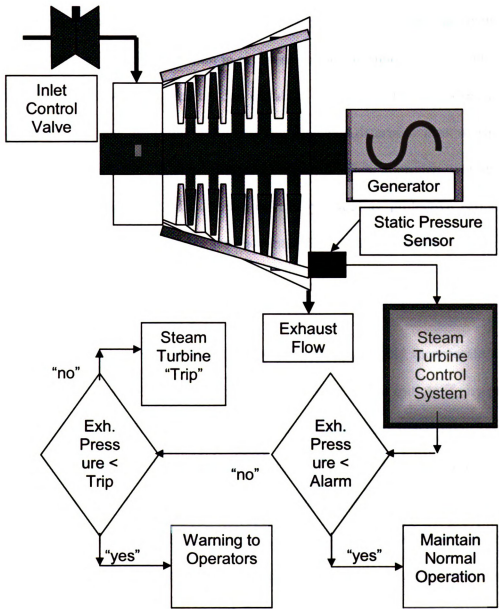


Figure 1.2 Steam turbine exhaust-pressure control system

A time dependent pressure signal obtained from these transducers can be converted into frequency domain using a Fast Fourier Transform (FFT) analyzer. The turbine control system takes this output and compares the pressure levels at various frequencies to a matrix of limiting values reflecting both alarm and trip signals. When one of the blade modes is excited, it results in variation in pressure on the surroundings of the blade. The dynamic pressure sensors can pick up this variation in pressure. It is proposed to relate these resonance frequencies to the pressure frequencies and determine a set of values for alarm and trip limits for different frequency ranges. This approach would enable operation over a wider range of exhaust-pressure by initiating protective actions only when unacceptable stress amplitudes are encountered as measured by the resulting local dynamic pressure pulsations.

The most basic system according to the proposed technique would incorporate a single dynamic pressure level. For example, the alarm could be set to initiate if any pressure level exceeds 0.5 psi. The trip set point would be determined based upon providing protection to the turbine blades, and could be set for 0.75 psi. It must be noted that the levels provided are reference values only. The actual frequency and pressure levels must be defined separately for each blade, based upon multiple factors such as material properties, blade stiffness, resonance characteristics, excitation sources and damping. Multiple dynamic sensors placed around the circumference of the turbine can provide increased reliability. A two-out-of-three type logic can be applied to prevent a protective response due to failure of a single sensor. The proposed technique can be used on any type of turbine with rotating blades and can be used to monitor real time vibration. It will

also be helpful in transient events such as during load rejection or breaker open event, when the steam is flowing through the turbine and generator is not producing any electricity. During this event, the exhaust-pressure rises and causes the steam turbine to trip. By the use of these sensors, the turbine can operate without tripping when there are no actual aerodynamics instabilities.

## 1.3    Objective and Goals

The main goal of this study is to develop a reliable and robust technique that can allow steam turbines to operate at wider operating ranges. An insight into the phenomenon of steam turbine exhaust-pressure is provided in this work. Various parameters contributing towards establishing the operating ranges of steam turbines are identified. A robust and inexpensive technique to monitor the vibration of the blades in real time is discussed. The use of dynamic pressure transducers to establish exhaust-pressure limits is suggested. The optimal locations of the pressure transducers in the turbine are identified. Extensive testing is performed in real steam turbine environment. The data is collected and analyzed to increase the operational flexibility of steam turbines. This research will benefit the industry to operate steam turbines more profitably and safely.

Many techniques have been developed over the years to understand the flow-induced vibrations. The main contribution of this dissertation is to allow the operation of a steam turbine to maximum capability of the last stage blade by allowing it to operate at higher than traditionally allowed exhaust-pressures. Another significant contribution is to present a reliable experimental technique that will help monitor the real time blade

vibrations by the use of dynamic pressure sensors. The data is used to define more realistic operational ranges of a steam turbine utilizing full capability of the last stage blades. The pressure variations are related to the maximum strain in the blade caused by various vibration modes. A thorough understanding of the flow distribution along the length of the blade is presented.

The method was assessed in the General Electric Company's new Low Pressure Development Test facility in Schenectady, NY. The low-pressure test turbine section is instrumented with both strain gauges on the blades to measure strain amplitudes and dynamic pressure probes in proximity to the tip of the blade to measure dynamic pressure response.

## 1.4    Outline of Thesis

This dissertation opens up with a detail discussion of fundamentals, hypothesis of operation, applications, limitations and challenges faced by steam turbine in chapter 2. Vibrations observed in steam turbine with a theoretical flutter model is discussed and stability regions have been identified. Chapter 3 discusses previous research on experimental techniques to measure aerodynamic instabilities. Chapter 4 describes selection and application of dynamic pressure transducers in Test 1. Test results are presented to help qualify the use of dynamic pressure transducers as a mean to measure blade vibrations. Chapter 5 discusses the details of experimental setup. Instrumentation locations and test plan were laid out. Chapter 6 provides the details of structural and modal predictions for the assembled row of blades. CFD analysis provides the flow

condition at the exhaust of the last stage blade. Allowable pressure and strain limits are described. Chapter 7 discusses test 1 and test 2 results comparison with analytical predictions. Chapter 8 provides conclusions for the research and suggestions for future work in this area.

# CHAPTER 2

# AERODYNAMIC INSTABILITIES IN STEAM TURBINES

## 2.1 Turbines

The word turbo or turbinis is of Latin origin and it means spins or whirls around. Turbomachines are devices in which energy is transferred to or from a flowing medium by the dynamic action of one or more moving blade rows. These rotating blades change the stagnation enthalpy of the moving fluid by performing positive or negative work that is caused by pressure change of the fluid. Turbomachines can be subdivided into two main categories: firstly those which absorb power by increasing the fluid pressure; secondly, those which produce power by expanding fluid to a lower pressure. Most common type of turbomachines includes compressors, pumps, turbines, propeller etc.

Turbines are used to generate power by converting thermal energy into mechanical energy. Various types of turbines were made more efficient with minimal losses to generate maximum output. The use of turbines as a part of power generation started in early 1900. In 1960's the steam turbines capacities grew steadily with higher steam temperatures and pressures. During 1970's the improvement in steam turbine design

10

increased the efficiency and reliability. After this, every component of the steam turbine has been studied extensively to improve the overall machine efficiency.

Highly specialized applications of the steam turbines, notably for geothermal and nuclear power plants got underway in the 1960s. The rebirth of the cogeneration and small power plants in the 1980s caused what could be described as scale down of the turbine technology. Advanced super critical steam cycles were applied to the steam turbines in 1950s.

## 2.2    Classification of Steam Turbines

Steam turbines are fundamentally classified as impulse and reaction type based on the way steam expands through a nozzle and impacts blade. Impulse stage can be compared to a waterwheel and the reaction stage to a rotary lawn sprinkler. In the former, for an impulse design, exhaust steam from one stage flows through similar impulse stages. The steam leaves the nozzles as well formed high-speed jets, which hits the moving blades thereby converting the steam's kinetic energy into shaft rotation. In the latter, the steam energy is absorbed in a series of constant pressure steps. In practice, steam turbines combine impulse and reaction stages.  The level of reaction on a stage can be defined in terms of enthalpy as

$$R = \frac{\Delta h_{rot}}{\Delta h_{stage}} \qquad (2.1)$$

Steam turbines come in an almost infinite range of sizes. Capacities ranging from 0.75KW to 1500MW for generator drive. They can be subdivided into two basic categories: condensing and non-condensing. In the case of condensing turbines, steam

11

leaves the turbine at a pressure below atmospheric. In other words, vacuum is maintained at the condenser so that steam can go into the condenser without any work loss. This is the most common type of turbine used to drive a generator to produce electrical power. In the non-condensing turbines the exhaust steam is used for industrial processes. The types of units have their widest application in process plants and are built to meet a wide variety of output requirements. Both condensing and non-condensing steam turbines are further categorized by the manner in which steam flows – straight flow, reheat, extraction, and induction. Straight flow uses full throttle steam flow from inlet to exhaust. In reheat units, virtually all of which serve for electric power production, the main steam flow exhausts from the unit at one (single reheat) or two (double reheat) intermediate stages. Temperature of the steam is increased before it is returned to the next lower stage for further expansion. Induction turbines work as extraction in reverse. These machines are generally found in the process plants.

Simple, small, multistage turbines are built with all the stages on a single shaft housed in one casing. With the increases in size, it becomes impractical to house all the stage in one casing. To avoid this, different stages are split amongst two or more casings on separate shafts. If all the shafts are bolted together to drive the same generator, this is called the tandem-compound unit. If the arrangements are such that two shafts or group of shafts are driving more than one generator, it is called cross-compounding.

Steam turbines function to accept high pressure and temperature steam for expansion through stationary and moving rows of nozzles and blades to convert heat energy into

mechanical (rotational) energy. Coupling with an electrical generator results in production of electric energy. It is common practice to include both gas and steam turbine to create a combined cycle. This configuration provides very high efficiency because the steam for the steam turbine can be produced from the thermal energy in the exhaust of the gas turbine.

## 2.3    Elements of Steam Turbines

Steam turbines are composed of hundreds of large and small components. Each and every part has its own importance and contributes towards the overall performance of the machine. An overall schematic diagram showing various components of a steam turbine is shown in Figure 2.1. Details of few major components are discussed below:

### 2.3.1  Blades or Buckets

Blades or buckets are the power producing components of a steam turbine. Primary function of the rotating blades is to transmit the working force of the steam as torque to the wheels and discs on which the blades are mounted. These aerodynamically designed vanes are subjected to unsteady steam forces during operation. As a result of these steam forces, the blades rotate the rotor shaft that is connected to the generator to produce electricity.
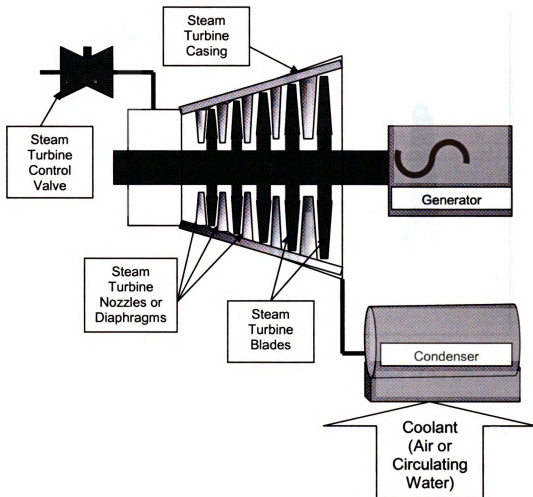
Figure 2.1 Schematic view of a power plant

|  |  |  |
|---|---|---|
| 40 in long last stage blade with curved axial type dovetail. | 27 in long blade with finger type dovetail. | 14.5 in long blade with pine tree type dovetail. |
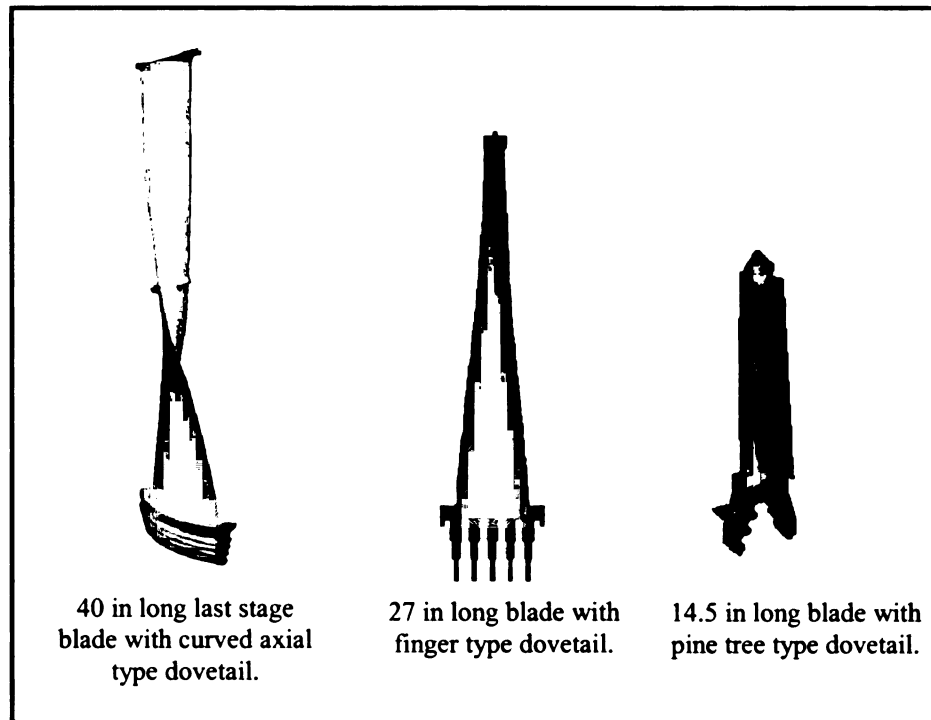
Figure 2.2 Examples of blades used in the low-pressure section of the steam turbine.

During the design of these components aerodynamic performance, stress distribution and frequency behavior are the most important considerations. In the modern turbines, due to requirement of high annulus areas, the last stage blades are becoming longer and their design is becoming more challenging. In order to provide stiffness and damping for an assembled row of blades, these blades have one or more connections along the length of the blade generally at the mid span and at the tip. A few typical blades are shown in the Figure 2.2.

## 2.3.2 Nozzle/Diaphragm

These are stationary components and the primary purpose of a nozzle is to accelerate and direct the steam flow to the rotating blades. The nozzles house in a semicircular ring and this ring also retains the packing rings to prevent steam leakage. A set of nozzle and blades make one stage. The nozzles contained in the diaphragms vary in size and passage area from stage to stage to efficiently handle the steam volume encountered at the various pressure levels throughout the turbine.

## 2.3.3 Rotors

Blades are attached to discs mounted on to a shaft, spindle, rotor, or drum. For smaller units, rotor with blades attachments may be machined from a single steel forging. As size increases, blades are attached to discs, which are either heat shrunk and keyed on to a forged and machined shaft or welded onto the rotor shaft. Large rotor may or may not have a central bore. In past years, bored rotors were necessary because of limitation of steelmaking capability. Stresses and imperfections tend to concentrate in the central bore region of the steel forging and the most practical way of dealing with them was to bore the rotor.

Bores also provided other advantages, such as inspection capability. Today even very large rotors can be made from a single forging. This rotor is called the monoblock. In addition, solid rotors can be welded together to form a single large rotor. Figure 2.3 shows a low-pressure section rotor with four blades stages mounted on it.
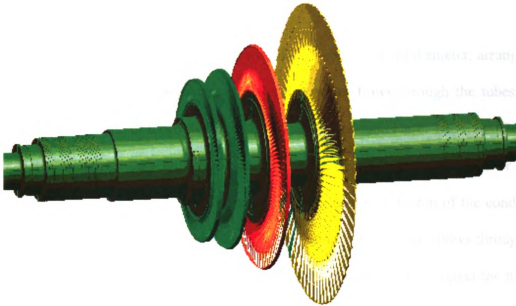
Figure 2.3 An assembled rotor with four rows of blades.

Drum type rotors, with a drum carried by the shaft, are common for turbines of largely reaction design. Diameters increase from the front to the rare end of the unit. The rotors are supported by bearings at each end.

### 2.3.4  Condenser

Once the steam has given up its energy to the turbine, it enters into the condenser. This steam coming out of the turbine is used to create vacuum at the exhaust of the turbine. In case if high condenser pressure, the steam has to push against the condenser pressure and this requires work. There are two main types of condensers: first type is known as jet barometric condenser in which water and steam come in direct contact.  In the second

type know as surface condensers, the steam and water remain separate, with indirect contact. Surface condensers are most commonly in the industry these days.

The design features a closed vessel filled with many tubes of small diameter, arranged in bundles and anchored by tube sheets. Condensing water flows through the tubes with steam contained by one or more shells on the outside of the tube bank. The water flowing through the condenser may be single-pass, or it may be made to reverse one or more times before being discharged. Turbine exhaust steam enters at the top of the condenser and passes down and around the tubes in the tube bundle. Cold water flows through the tubes to condense the steam. It is then returned to the cooling tower to reject the heat of condensation. The condensed steam is recovered as water and pumped back to boiler.

## 2.4 Limitations and Challenges

Steam turbines have been used for power generation for more than a century. Competitive market demands are driving for turbines with higher efficiency and reliability. With these demands, the design of the steam turbine is becoming challenging and turbines are required to operate at higher than traditional allowed operational limits. Operating limits are defined for the safety and reliability of the steam turbine itself and for the safety of the people working around it. The factors that are commonly used to set these operational limits are vibration levels at various locations on the turbine, temperature, pressure, speed of turbine etc. Exhaust-pressure limits are primarily defined to provide safety to the last stage blades of the low-pressure section of the steam turbine. This is one of the biggest limiting factors in the operation of the steam turbine. This

dissertation is focused on understanding the consequences of operations at higher exhaust-pressures and provides a technique that can be used to alleviate the problems associated with operation at higher exhaust-pressures.

## 2.5    Vibrations in Turbine Blades

Rotating blades of turbines are subjected to a variety of steady state and transient loads. These loads can excite one of the fundamental vibration modes of the assembled row of blades. Since almost all the blade failures are caused by vibratory stresses, blade designers try to avoid all possible resonances by detuning the blades. Frequency tuning becomes more challenging with increasing length of the blade as in the case of the last stage blades of the low-pressure section of the steam turbine.

The vibrations observed in the steam turbines blades can be divided into two distinct categories: synchronous and non-synchronous vibrations. Synchronous vibrations are excited at integer multiples of the shaft rotation frequency caused by nozzle excitations, rotor imbalances, non-concentric casings and pressure fluctuations. Non-synchronous vibrations or flow-induced vibrations are caused by aerodynamics instabilities created by steam flow. An important feature of the non-synchronous vibrations is that the frequency-speed characteristics do not "ride" on the engine order line. As the response departs from the engine order line, the potential of aerodynamics instability can be high. Flow induced vibrations is the main focus of this study and will be discussed in the following section.

For the case of synchronous vibrations, the major source of excitation of the natural frequencies is the excitation in the nozzles. The frequency of the nozzle excitation forces is a function of the number of nozzles and the speed of the turbine. These excitations are due to the reduced velocity at the wake (trailing edges) of the nozzles. The force experienced by the blade depends upon its relative position with respect to the nozzle in one complete revolution.

## 2.5.1 Blade Vibration Mode Shapes

Mode shape is defined as the deflected shape of a structure at one of its resonance frequency. For any structure in resonance, there are points on the structure that remain stationary. In the case of row of blades, these points fall either on a nodal line or on a circle. The modes shapes of a row of blades are characterized by specifying these nodal lines or nodal circles. The mode shapes are also designated by the direction of motion of the blades i.e. axial, tangential and torsional. Figure 2.4 shows few mode shapes of an assembled row of blades.
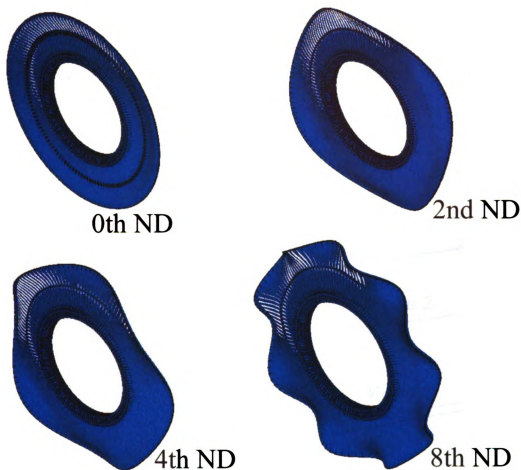
Figure 2.4 Typical mode shapes of a row of blades, showing 0, 2, 4 and 8th nodal diameter.

## 2.5.2 Campbell Diagram

A Campbell diagram is a graph with turbine speed (rpm or rps) plotted on the horizontal axis and frequency (Hz) plotted on the vertical axis. Also drawn are the blade frequencies and stage exciting frequencies. When a blade frequency and an exciting frequency are equal or intersect, it is called resonance. Modes are drawn on the Campbell diagram by joining these resonance points. This plot shows an overall frequency response of the

blade at different speeds. Speed and frequency margin are calculated for the speed of interest. Every manufacturer has their design rules specifying the allowable minimum margins for each engine order. Figure 2.5 shows a typical Campbell diagram.
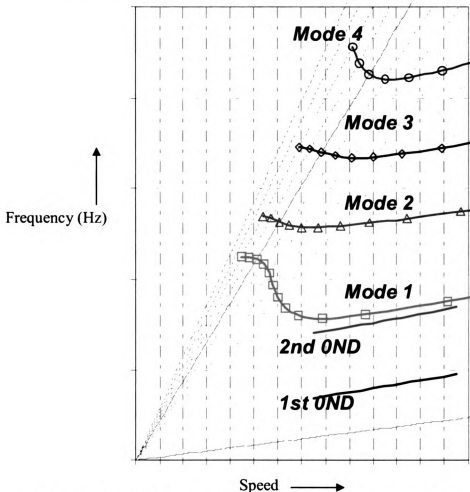


Figure 2.5 Typical Campbell diagram with various vibration modes.

### 2.5.3 SAFE or Interference Diagram

The Campbell diagram is a two dimensional projection of a three-dimensional surface; hence, it does not retain all the information for evaluation. Another two-dimensional projection of the same surface contains more information for easier evaluation. This other two dimensional graph is called as SAFE or interference diagram. On the Interference

diagram, mode shape or nodal diameters are drawn on the horizontal axis and frequency on the vertical axis. This plot provides the vibration information at one speed. Different modes and the speed lines are plotted on the graph. Interference plot shows, if there is a crossing of any mode with the speed line at any nodal diameter. Figure 2.6 shows a typical Interference diagram.
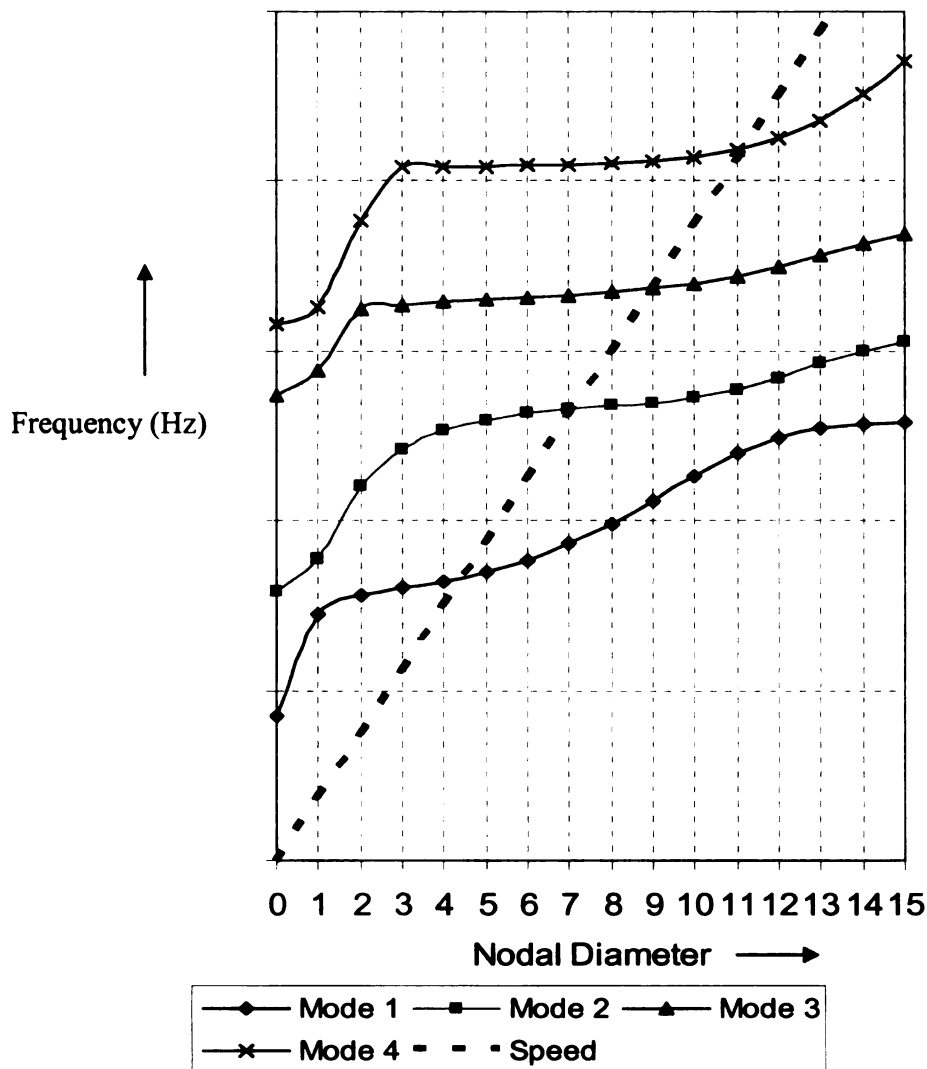
Figure 2.6 Typical Interference diagram with various vibration modes

## 2.6 Flow Induced Vibrations

In order to understand fundamentals of aerodynamics instabilities, consider a structure with noncircular cross section in a flow field. It experiences a fluid force that changes with orientation to the flow. At higher velocities, as the fluid transitions to the turbulent region, a pattern of vortices is formed at the trailing edge of the body. These vortices interact with the body and are the source of vortex-induced vibration. If the oscillating fluid force tends to increase vibration, the structure is aerodynamically unstable and very large amplitude vibrations can result. Forcing functions due to periodic synchronous disturbances in the steam flow can excite the blades in the fundamental modes. However, the blades may be subjected to non-synchronous vibrations due to self-excited mechanisms created by steam flow such as Buffeting, Stall Flutter etc. A helpful overview of this phenomenon is presented by Blevins [9].

*Buffeting* occurs at low flows and at high exhaust-pressure conditions. Generally this is regarded as response to a random forcing function [8] similar to the lift exerted upon an airfoil moving in a turbulent moving fluid. Although last stage blades respond to buffeting to some extent but is not a limiting factor if operated within "safe" exhaust-pressure range. At high exhaust-pressure and low load, the incidence of the approaching flow is such that the lift of the rotating blades is alternately lost and restored as the blade deflects.

*Un-stall flutter* occurs at design or near design conditions and is most likely to occur at maximum load. Analytical predictions have shown that at certain inter-blade phase angles,

24

the unsteady aerodynamic forces will reinforce the blade vibration resulting in sufficiently high response that may lead to blade failure [4]. Un-stall flutter has not been observed in the steam turbine.

*Stall Flutter* occurs at low flow and high exhaust-pressure operating conditions. Vibration amplitudes are generally very high and onset of the vibration is explosive. Free standing and welded construction are most susceptible to this type of flutter.

For steam turbines, Buffeting and Stall Flutter are the greatest perceived risks that tend to restrict the operational limits. In assembled turbine blades, the welded type construction, due to rigid structure are more prone to Stall Flutter and continuously coupled type blades are more affected by Buffeting. Figure 2.7 shows the response from strain gauges placed at blade vane roots during field tests plotted verses average exit velocity of steam. As shown in the plot low annulus velocities show higher strain amplitudes.

As the fluid exerts a force on the structure, the structure exerts an equal but opposite force on the fluid. The force of structure on the fluid can synchronize with vortices in the wake and produce large amplitude vibrations. At higher Reynolds numbers, the vortices form and shed alternately from side to side. Such periodic behavior gives rise to a periodic force on the object and if the coupling occurs with the mechanical system, a self-sustained oscillation may result. Resonance conditions may cause catastrophic failure. Flow separates from the back of a body at Reynolds number greater than 50, based on the width of the body.
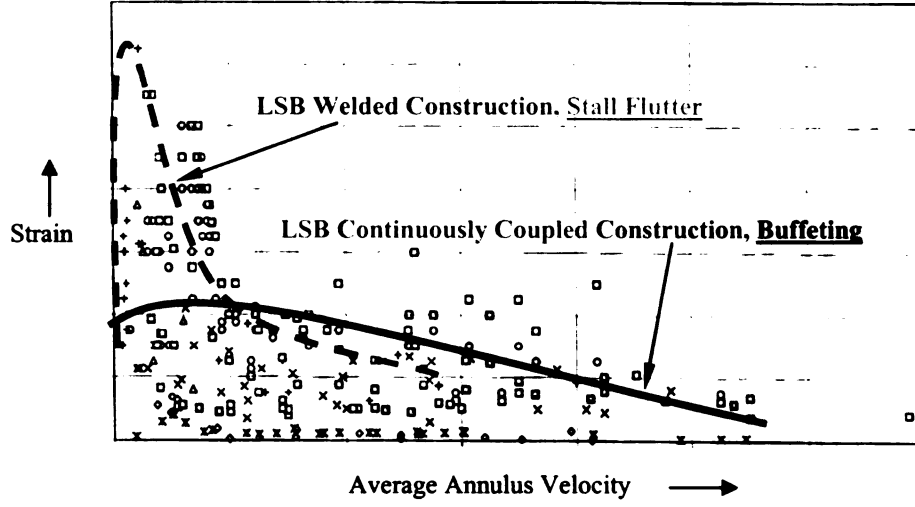
Figure 2.7 Last stage blades response against average annulus velocity.

## 2.7 Flutter Modeling

Various attempts have been made to mathematically model the flutter conditions using simple airfoil geometry. Belvins [9] has summarized the work in concise manner. Consider an airfoil section supported by two springs providing stiffness in the vertical and torsional directions as shown in Figure 2.8. The equations of motion for this section can be written as

$$m\ddot{y} + 2m\zeta_y\omega_y\dot{y} + S_x\ddot{\theta} + K_y y = F'_y \tag{2.2}$$

$$J_\theta\ddot{\theta} + 2J_\theta\zeta_\theta\dot{\theta} + S_x\ddot{y} + K_\theta\theta = F'_\theta \tag{2.3}$$

Where y is the displacement in vertical direction at the elastic axis (positive downward) and θ is the twist (positive clockwise). Mass of the section and mass moment of inertia can be approximated as that of a flat plate.

$$m = \frac{\rho \, \pi \, c^2}{4} \qquad (2.4)$$

$$J_\theta = \frac{\rho \, \pi \, c^4}{128} \qquad (2.5)$$

Lift, drag and moment forces per unit span can be expressed as a function of lift, drag and moment coefficient as

$$F_L = \frac{\rho U^2 c C_L}{2} \qquad (2.6)$$

$$F_D = \frac{\rho U^2 c C_D}{2} \qquad (2.7)$$

$$F_\theta = \frac{\rho U^2 c^2 C_M}{2} \qquad (2.8)$$



**A.C.   Aerodynamic center**
**C.G.   Center of gravity**
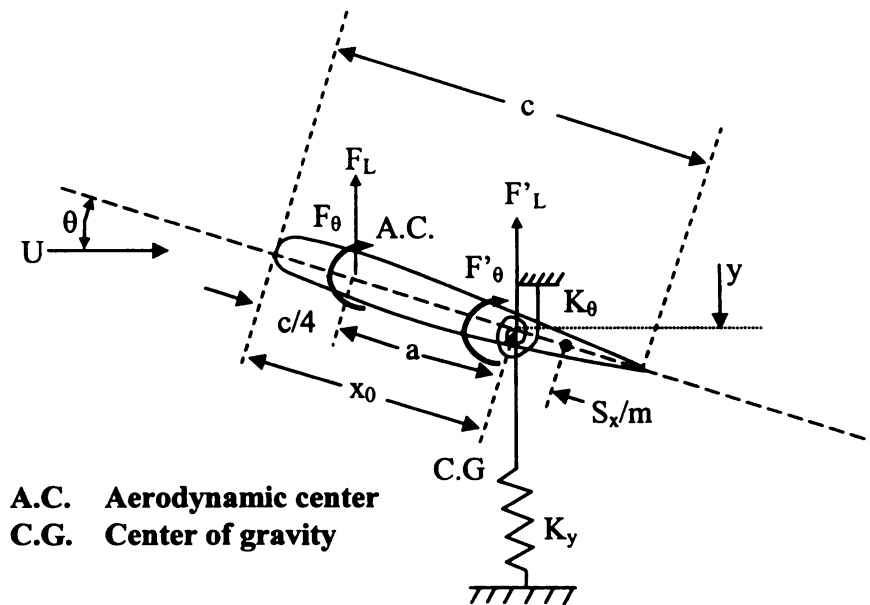
Figure 2.8 Two-dimensional airfoil section supported by vertical and torsional springs.[9]

27

The angle of attack ($\theta$) has great impact on the magnitude of these forces. At large angles the flow separates from the back of the airfoils and drag increases sharply while lift decreases. This condition is called as stall or separated flow condition. For an angle of attack between $\pm 8°$ the coefficients of lift, drag and moment are

$$C_L = 2\pi \ Sin\theta \qquad C_D \ \& \ C_M = \text{order of } 0.01 \qquad (2.9)$$

Net vertical force applied on an airfoil is a sum of lift and drag forces vectors in the vertical plane. At small angles of attack, the drag force is very small as compared to the lift force so an approximation can be made as

$$F_y' = F_y \approx -F_L \qquad (2.10)$$

Negative sign is due to sign convention as positive lift upward. The aerodynamic moment is generally referenced to the aerodynamic center. The moment at the elastic axis is the sum of the moment at the center and moment induced by the offset (a). The moment at the aerodynamic center is smaller as compared to the moment due to lift.

$$F_\theta' = F_\theta + aF_L \approx aF_L \qquad (2.11)$$

For static flutter stability, ignoring the time derivatives terms in equations 2.2 & 2.3 and substituting equations 2.6 through 2.11 with the assumption of small angles

$$y = -\frac{\pi\rho U^2 c\theta}{K_y} \qquad (2.12)$$

$$(K_\theta - \rho U^2 ca\pi)\theta = 0 \qquad (2.13)$$

The equilibrium solution $y = \theta = 0$ is stable if the quantity in the parentheses in equation 2.13 is positive. If the flow velocity is increased to the point where the quantity in the parentheses becomes zero, large torsional deformations will results from slight perturbations. This is called as divergence and it occurs at the divergence velocity

$$U_{diverge} = \sqrt{\frac{K_\theta}{\pi \rho c a}} \qquad (2.14)$$

Above equation provide the static stability condition.

## Stall Flutter:

We can examine the stability conditions by considering vertical and torsional motion separately. For the case of plunge motion only, the equation of vertical motion (2.2) with $\theta = 0$ for small angles can be written as

$$m\ddot{y} + 2m\zeta_y \omega_y \dot{y} + K_y y = -\frac{\rho U c}{2}\left(\frac{\partial C_L}{\partial \alpha} + C_D\right)_{\alpha=0} \dot{y} \qquad (2.15)$$

For stability $\frac{\partial C_L}{\partial \alpha} + C_D > 0$ and at small angles $\frac{\partial C_L}{\partial \alpha} = 2\pi$ and $C_D > 0$. If the angles exceeds $\pm 8°$, lift decreases ($\frac{\partial C_L}{\partial \alpha} < 0$ ) and an instability called stall flutter will occur.

Considering only the torsion displacement and with y=0, Fung [11] presented the equation of motion of torsion with quasisteady aerodynamic forces as

$$J_\theta \ddot{\theta} + 2J_\theta \zeta_\theta \dot{\theta} + K_\theta \theta = \frac{\rho U^2 c^2}{2}\left(\frac{x_0}{c} - \frac{1}{4}\right)\frac{\partial C_L}{\partial \alpha}\theta - \frac{\rho U c^3}{2}\left[\frac{\pi}{8} + \left(\frac{x_0}{c} - \frac{1}{4}\right)\left(\frac{x_0}{c} - \frac{3}{4}\right)\right]\dot{\theta}$$

$$(2.16)$$

The quantity in the square brackets is always positive, the aerodynamic moment proportional to angular velocity provides aerodynamic damping. Thus the aerofoil is

dynamically stable in torsion but is statically unstable in torsion if the velocity exceeds the divergence velocity shown in equation 2.14.

## Classical Flutter:

The airfoil can also become unstable in coupled torsion-plunge (vertical motion) mode known as classical flutter. Ignoring damping, and assuming vertical force is caused by lift force only, equations 2.2 & 2.3 can be written as

$$m\ddot{y} + S_x\ddot{\theta} + K_y y = -\frac{\rho U^2 c}{2}\left(\frac{\partial C_L}{\partial \alpha}\right)\theta \qquad (2.17)$$

$$J_\theta\ddot{\theta} + S_x\ddot{y} + K_\theta\theta = \frac{\rho U^2 ca}{2}\left(\frac{\partial C_L}{\partial \alpha}\right)\theta \qquad (2.18)$$

Assuming a solution $\qquad y = A_y e^{\lambda t} \qquad \& \qquad \theta = A_\theta e^{\lambda t}$

Where $\lambda$, $A_y$ & $A_\theta$ are constants and t is time. By substituting the assumed solution in equation 2.17 & 2.18, we get

$$\begin{bmatrix} m\lambda^2 + K_y & S_x\lambda^2 + \dfrac{\rho U^2 c}{2}\left(\dfrac{\partial C_L}{\partial \alpha}\right) \\ S_x\lambda^2 & J_\theta\lambda^2 + K_\theta - \dfrac{\rho U^2 ca}{2}\left(\dfrac{\partial C_L}{\partial \alpha}\right) \end{bmatrix}\begin{pmatrix} A_y \\ A_\theta \end{pmatrix} = 0 \qquad (2.19)$$

A polynomial solution to the equation 2.19 can be obtained by putting the above determinant to zero as

$$C_0\lambda^4 + C_2\lambda^2 + C_4 = 0 \qquad (2.20)$$

Where $\qquad C_0 = mJ_\theta - S_x^2$, $\qquad C_4 = K_y\left[K_\theta - \dfrac{\rho U^2 ca}{2}\left(\dfrac{\partial C_L}{\partial \alpha}\right)\right]$

$$C_2 = m\left[K_\theta - \frac{\rho U^2 ca}{2}\left(\frac{\partial C_L}{\partial \alpha}\right)\right] + K_y J_\theta - \frac{\rho U^2 c}{2}\left(\frac{\partial C_L}{\partial \alpha}\right)S_x$$

An exact solution to this problem is

$$\lambda = \pm\sqrt{\frac{-C_2 \pm \sqrt{C_2^2 - 4C_0 C_4}}{2C_0}} \qquad (2.21)$$

There are four roots, some of which will be complex. $C_0$ is always positive as $J_\theta \geq S_x^2/m$ and $C_4$ is always positive for velocities below onset of divergence. Only the values of $C_2$ are of consequence of flutter. If $\lambda$ have negative real parts, small perturbations will decay in time. If $\lambda$ have positive real parts, perturbations will grow in time. To determine onset of flutter, Pine et al. solved the above equation at $\lambda=0$ Pines [10] solved the above equation that produces the onset of flutter as

$$\left.\frac{\rho U^2}{2}\right|_{flutter} = \frac{[-E \pm \sqrt{(E^2 - 4DF)}]}{2D} \qquad (2.22)$$

Where

$$D = \left[(ma + S_x)c\frac{\partial C_L}{\partial \alpha}\right]^2, \quad F = (mk_\theta + K_y J_\theta)^2 - 4(mJ_\theta - S_x^2)K_y K_\theta$$

$$E = [-2(ma + S_x)(mk_\theta + K_y J_\theta) + 4(mJ_\theta - S_x^2)aK_y]c\frac{\partial C_L}{\partial \alpha}$$

A flutter situation can occur when one of these terms is real and positive. At the onset of the flutter, the natural frequencies of torsional and plunge modes combine to form a single frequency-coupled mode that does not exist without flow. Flutter is dependent

31

upon geometric relationship between aerodynamic center, elastic center and center of mass. Flutter can be prevented if the center of mass is forward of the elastic center. Other features that influence flutter includes damping, mass, stiffness and airfoil contours.

# Chapter 3

# Literature Review

Reliability of rotating blades is critical to the availability and safety of power generation industry. Large last stage blades are highly stressed complex structures, which must tolerate a verity of loads in an adverse environment. The main reason of this can be attributed to the blade failures caused by vibration fracture. During the design phase, rigorous vibration testing is conducted in the factory to determine the vibration response of the blades and in the field many techniques have been developed to capture the vibrations of the blades in real steam environment.

## 3.1 Existing Techniques for Turbine Blade Data Acquisition

Many techniques have been developed to understand the phenomenon of non-synchronous vibrations in the history of steam turbine research. Main objective of all of these techniques was to measure the frequency and amplitude of blades in resonance. It is easy to measure the vibration characteristics of the blades in the factory environment but become challenging in enclosed and wet field environment. Following are the techniques that were used to acquire the vibration data of the blades.

### 3.1.1 Strain Gauges Based Measurements

The most accurate method of determining the mode shapes and frequency of vibrating blades is the use of strain gauges. Strain gauges methods involve the attachment of several strain gauges to various critical blade areas, with the associated instrumentation connected to the rotor itself. These are now well established and field proven systems for obtaining information relating to the alternating strains arising in certain critical areas of the blades but there are significant inherent problems associated with such systems. The limited life of the gauges, connecting wires and associated instrumentations due to environmental influences such as unsteady pressures and large centrifugal forces pose serious problems.

One of the major problems, however, is related to the need to transmit the signals from the rotating structure to the stationary analysis hardware. Slip-ring or telemetry systems are usually employed, but installation is difficult, invasive and/or expensive. Moreover they are often a considerable source of noise. In addition, the wire paths can alter the blade structural characteristics as well as interfering with the local fluid flow field. Therefore the use of strain gauges is restricted to a few blades per rotor stage. Strain gauge based measurements are therefore part of a test method that can produce extremely valuable information on certain parts of the blade, but are statistically unreliable due to the irregularity of the blade tolerances. The biggest problem in use of strain gauges in steam turbine is the life of the transducers in harsh wet environment.

## 3.1.2 Frequency Modulated Grid Measurements

In frequency modulated grid measurements, the amplitude of the blade tip vibration is measured [21]. A small permanent magnet attached to the blade tip induces an alternating electromagnetic voltage in a winding installed in the machine casing. Any oscillating vibratory motion of the tip as it rotates modulates the AC voltage curve, and can be resolved by filtering or more usually by frequency analysis.

Clearly, one limitation associated with this technique is that only one blade can be monitored at a time with a full winding or a small number with partial windings. The major problems, however, are the considerable, high cost modifications that are necessary to incorporate and support the windings in the casing, and the fact that the magnets installed at the tip must withstand large centrifugal forces. With this technique, it is also difficult to detect the modes that have small or no motion at the tip of the blade.

## 3.1.3 Laser Doppler Vibrometry

Laser Doppler Vibrometry (LDV) relies on the detection of the Doppler frequency shift in light scattered from the moving target [2]. By measuring this frequency shift, a measurement of the target velocity is obtained. Careful selection of the location of an optical window in the casing can help in getting vibration information of any point of blade surface as well as the tip. The non-contact nature of the LDV offers significant advantages over the traditional contact vibration measurements systems.

LDV based vibration measurements on the rotating targets can be performed in two distinct ways [14]. The "Eulerian" approach, in which the LDV obtain a measurement of component vibration as the target passes through the laser beam. In the second approach called as "Lagrangian" approach, some form of beam steering device is used, such as a rotating mirror to track the particular point of interest on the rotating blade. One drawback in the use of LDV is the cost and for the steam turbine, the presence of moisture at the last stage makes this application difficult.

## 3.1.4 Non-Contact Blade Vibration Monitoring System

Non-contact blade vibration measurement is another technique that is becoming very popular. Vibrational tip deflections are deduced from measurement of the times at which the rotating blades pass stationary sensors [7]. Generally two sensors are sufficient to measure non-synchronous vibration, but multiple sensors are required to characterize synchronous vibration. These sensors are mounted in the vicinity of the blade covers targeting some prominent feature of the cover.

Hu et al. [13] presented a two-sensor working principal. The basic principal of two-sensor method is based on the fact that the passing time, during which a vibrating blade covers the circumferential separation distance between the two sensors, is different from the passing time in the absence of blade vibration. In the absence of the blade vibration, the passing time is determined by rotor rotational speed only, whereas in presence of vibration, the passing time depends on the amplitude and frequency of the vibrating blade.

Assuming a constant rotor speed, the difference of the momentary deflection of the blade tip at the two sensors can be determined with the equation

$$\Delta y(n) = \Delta t(n) \times u(n) - b \qquad (3.1)$$

Where $\qquad\qquad\qquad u(n) = \Omega(n) \times R$

The blade vibration amplitude and frequency can be extracted from the spectral analysis based on the differences of the momentary vibration deflection in several revolutions. Figure 14 shows a schematic diagram of the two-sensor method.
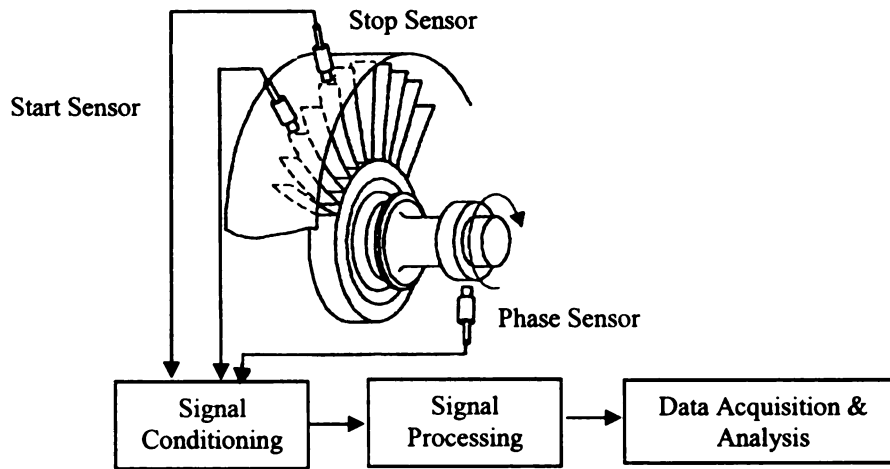


Figure 3.1 Setup for the non-contact blade vibration monitoring system. [13]

Two magnetic sensors are mounted in the machine casing along the circumferential path above the blade tips to sense the blade passing time of each blade. Rotor speed can be measured using a phase sensor placed on the rotor. It is good to have the phase sensor close to the last stage blade to reduce rotor torsional effects. Using the information collected from this test, circumferential vibration amplitude can be calculated as

$$a_u = \Delta y_{\max} /(2\sin(\pi\omega \ z_b/\Omega \ z)) \qquad (3.2)$$

The maximum local blade stress can be correlated with the circumferential vibration amplitude with the prior knowledge of blade natural vibration mode shapes or by strain gauge measurements. Prior knowledge of blade natural frequency can help avoid aliasing frequencies. Finite element analysis techniques can be used to predict natural frequencies of a row of blades.

This technique can be applied to detect both synchronous and non-synchronous vibrations. In the case of synchronous vibration, a blade tip follows exactly the same path each time the blade rotates. Stationary sensor can easily detect the same arrival time relative to the shaft position. Although, in the case of non-synchronous vibration, the arrival time of blade may not be same for each rotation, but a two-sensors system can be used to detect these vibrations. The amplitude of the vibration can then be compared to the limiting amplitudes to define an alarm and a trip limit.

Few limitations with this technique are

1. Due to typical bending and torsion vibration of twisted blades, the exact knowledge of the actual axial sensor position over the blade tip is required.

2. In order to avoid aliasing due to noise and response due to higher modes, filtering before sampling is required.

3. Another limitation is that only the vibration modes with tip displacement can be detected.

Non-contact blade vibration measurement can also be used to detect rotor torsional vibration. Measurements can be made at any location at the rotor where sensors can detect appropriate targets.

## 3.2    Flow Induced Vibrations

As mentioned before, the blade designer can control synchronous vibration excitation by tuning the blades, but he has very little control on the non-synchronous vibrations. Some effort has been made to understand this phenomenon and a very limited amount of published experimental analysis has been reported in literature on aerodynamic instabilities in steam turbine. This section will summarize the work that has been done in this area.

In an instability condition, the aerodynamic forces induced due to blade vibration feed energy into the structure, and thus stresses escalate with each additional cycle of vibration. The chances of exciting these high magnitude oscillations can be higher as the turbine operation departs from the engine order-lines [3]. The only mechanism that limits these non-synchronous vibrations (by dissipating energy) are the material, structural and aerodynamic damping. Lazan [6] has presented a method to estimate material damping knowing the magnitude of steady and dynamic stresses.

Evans and Wang [4, 5] used aerodynamic damping to predict the stability operating regions. An estimate of aerodynamic damping is made using unsteady compressible

Navier-Stokes equation. Wang [5] has observed the chances of aerodynamics instabilities to occur at very high mass flow rates as well as at very low rates with higher exhaust-pressures. Generally the plant operators do not operate in region with high mass flow rates due to unavailability of more steam and restrictions applied by the manufacturer. Evans [4] has presented experimental data on the relationship between inlet density and the blade response. Blade response rises rapidly over a small range of densities, which would be expected, from the un-stall predictions. High responses have been observed with increasing steam density. Figure 3.2 shows the blade response vs. steam density at different moisture levels.
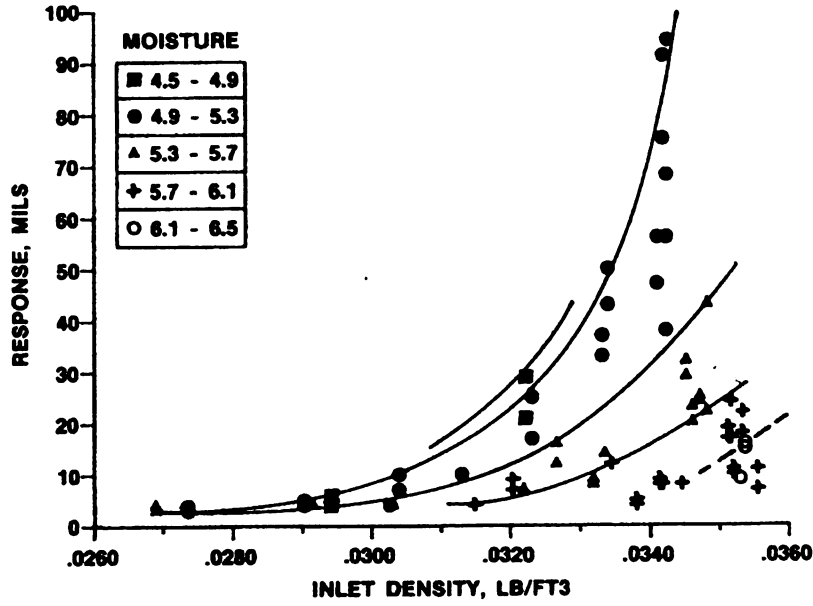


Figure 3.2 Strain gauge responses vs. density plot at different moisture levels. [4]

Evans [4] also showed the impact of mix-tuning (mistuning) to alleviate the susceptibility to un-stall flutter. Mix-tuning was achieved by installing blades in a pattern such that

40

alternate blades have natural frequencies different from each other. In order for flutter to be maintained, the blades must be vibrating at the same frequency. Having adjacent blades at difference frequency reduces the susceptibility to flutter.

Bell [16] used pressure transducers in a cascade on a single blade to measure the pressure distribution around the blade. These externally mounted pressure sensors measured the pressure signals from the blade surface. The work was focused on addressing the influence of tip clearance upon the local unsteady aerodynamics of oscillating blades. The results showed a consistent variation in amplitude of the unsteady pressure response at 90% span for change in tip gap. Queune et. al [17] studied the response from oscillating blade under massive tip separation. The experimentation was conducted in a cascade using a single blade. Pressure transducers were used to measure the pressure variations around the blade surface. To understand flutter problem, He [18] performed experiments in a cascade with 7 blades. The middle blade was forced to oscillate using a motor. Pressure distribution around the blade was measured using pressure sensors. The results showed effect of bubble type separation on the unsteady pressure, which mainly resulted from the movement of the transition points.

Truckenmuller et. al. [19] conducted experimental investigation of dynamic loading of the running blades in three-stage low-pressure steam model turbine. The pressure distribution for every stage was measured with static pressure taps in the steam flow paths. The purpose of the study was to understand the dynamic loading caused by excitation by individual modes on each stage.

Flow reversal in the hub region of the last stage rotor blade of steam turbines is an observed phenomenon occurring at low mass flow [20]. Along with this flow reversal comes increased blade path temperatures as the turbine blade path acts as a compressor-delivering energy into the working fluid. The almost worst case occurs at design speed and even worst at overspeed condition with zero mass flow rate. For large steam turbines, windage power levels can be on the order of two to three thousand kW depending upon the steam pressure levels. Other concern with the flow reversal is the erosion indication on the tip inlet and hub exit region of the last stage blade. Steltz [20] presented the flow reversal as a function of exhaust volumetric flow rate. Figure 3.3 shows the volumetric flow rate plotted vs. blade reversal height ratio.

## 3.3 Conclusions

In the past 50 years, a lot of efforts have been made to understand the aerodynamics instabilities caused by flow-induced vibrations. Designers have been successful in controlling the synchronous vibrations by properly detuning the blades but have very little control on the non-synchronous vibrations. Most of the work on non-synchronous vibrations, available in the literature, is in the area of aircraft engines and gas turbines. Limited amount of experimental and theoretical published work is available in steam turbine area.

42
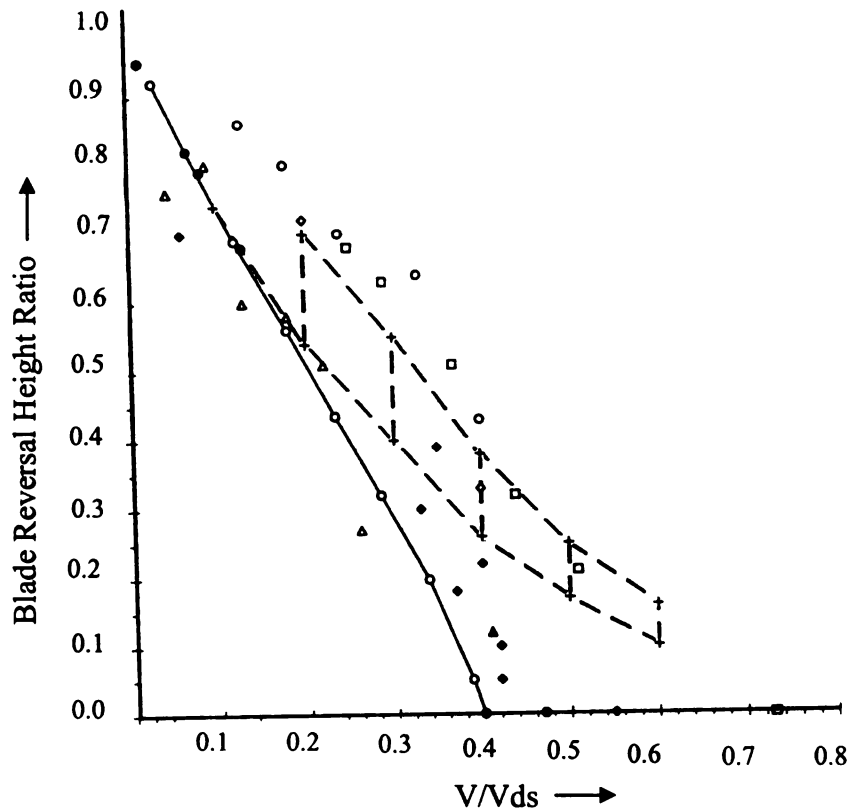
Figure 3.3 Flow reversal at the hub as a function of exhaust flow rates. [20]

Drain (1980), Rozelle and Hu (2002) have presented experimental techniques to capture vibration information of the rotating blades. All these methods have their limitation on application in the real steam environment. Queune (2001), Bell (2000), Steltz (1999), He (1998) and Truckenmuller (1998) have studied various parameters that influence flutter. Belvins (1990) have presented techniques that can be applied for mathematical modeling of the flutter.

In the work reported in literature, most of the experimentation is performed in cascade with simplified turbine configurations and air is used as an exciting medium. Very few results are available from actual steam turbines. Steam has diverse chemistry and can

interact with blades differently as compared to air. Also the experimental results obtained from cascade can be misleading as the operating conditions are not the same as that of an actual steam turbine. Only a test on a steam turbine can provide the results with highest level of accuracy.

The technique presented in this dissertation is inexpensive and is capable of capturing any type of vibrations in the blade. The biggest contribution is that the validation of this technique is done in the real steam turbine environment. Detailed study of the flow field is done with strain gauges, static and dynamic pressure sensors mounted in steam path and on the blades. This work will contribute towards the information collected from the real steam turbine environment

# Chapter 4

# Dynamic Pressure Transducers

The biggest challenge in use of dynamic pressure transducer was to find the appropriate transducers that can operate satisfactorily in steam environment. Application of the pressure transducers in steam turbine presents certain challenges and constraints. There are various factors such as proper sealing for moisture, corrosion etc. that needs consideration for application in such environment. Proper orientation and location of pressure transducers is critical for getting accurate response.

## 4.1    Selection Criteria

Dynamic pressure transducers are used to measure variations in pressure caused by moving fluids. These transducers sense any change in pressure amplitude in their surroundings. Dynamic pressure transducers are made by various manufacturers and are available in different sizes, pressure ranges, application temperature range and sensitivity levels. The transducers are housed in probes and two different probe types were used for this test.  Type 1 has the transducer recessed inside a tube with a side hole port to the transducer.   Type 2 has the transducer mounted at the end of the probe.   Dynamic pressure transducers were placed on the traverse and on the steam guide. Travers consists

45

of a probe carrying the transducers and can move along the radial height of the blade, whereas the steam guide is located downstream of the last stage blade and it guides the steam into the condenser. For use on traverse, Type 1 was preferred because it can be rotated with an attempt to obtain static and total pressure readings along with dynamic readings. For use on steam guide, type 2 probes were selected.

As mentioned before, the main objective of test 1 was to check the survivability of the dynamic pressure transducers in the wet steam environment. Following selection criteria were used in selection of these transducers

- Size of the Transducer

- Pressure Range

- Application Temperature

- Hermetic Sealing

- Sensitivity

## 4.2 Limitations

One limitation in the use of dynamic pressure transducer is the moisture content in steam at the last stage blade. If the dynamic pressure sensors are not properly sealed, moisture can penetrate into the transducer, which can lead to incorrect response or to transducer failure. Other limitation in steam is the erosion due to moisture. These limitations can be addresses by selecting the appropriate material transducers that are hermetically sealed.

On steam turbines, generally at the exit of the last stage blade cooling sprays are provided. Water is sprayed to keep the temperature down at the exhaust of the last stage blade during protracted no load conditions. Incorrect location of the pressure transducers can result in submerging of transducers under a layer of water.

## 4.3  Application

Special probes were designed to carry the dynamic pressure transducers on the traverse. The traverse probes were 102.5 inches in length comprising of a 97.5 inch length with 0.5 inch diameter and a 5 inch length with 0.25 inch diameter. The purpose of having two tubes was to provide damping at resonance conditions. Vibration test was conducted to verify the natural frequencies of the probe. The design intent was not to excite the probe due to flow stimulus. Figure 4.1 shows the schematic of probe with transducer. Figure 4.2 shows the probe installed on the turbine.
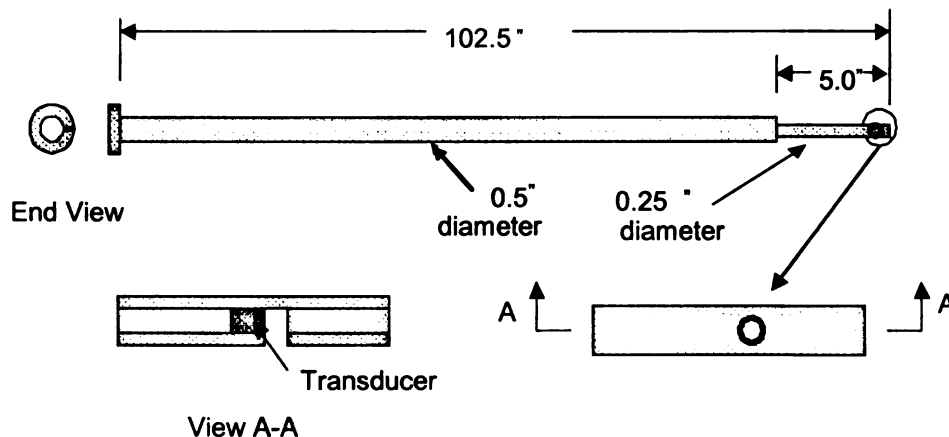


Figure 4.1   Probe and transducer configurations

47

### 4.3.1 Transducer Orientation

In test 1 , the dynamic pressure transducers were placed only on the traverses and the data were collect by traversing in radial direction and holding the sensors at 25%, 65% 80% and 90% radial locations. Riaz et. al. [1] has provided a through detail of this.



Figure 4.2   Probes mounted on the turbine.

At each radial location the sensors were rotated around 350° degrees to fully capture the flow characteristics.  In the test, steam mass flow was constant but the exhaust-pressure was raised up to 51 kPa (~15 in HgA). Introducing a controlled amount of atmospheric

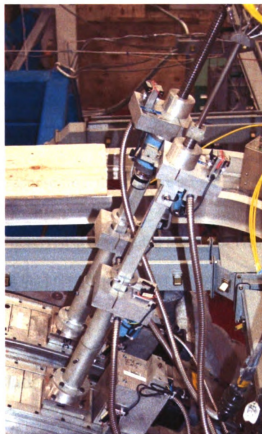air in the condenser from surroundings raised exhaust-pressure in the condenser. Figure 4.3 shows the pressure amplitude changing as the traverse rotate at 90% radial location. At around 135° location, the pressure sensor was facing the flow and maximum pressure is observed at this location.
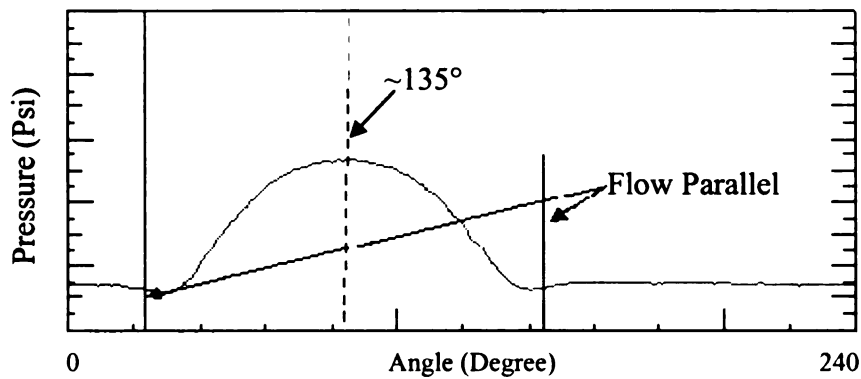


Figure 4.3 Response from the pressure sensor at 90% radial location.

Similar responses were observed at other radial locations. This part of the test provided an optimal orientation of the pressure transducer where best response was observed.

## 4.3.2 Individual Blade Tracking

An important consideration in using pressure transducer was the ability of the transducer to sense the pressure pulsation caused by vibrating blades. To check this, the data from the test was analyzed to see if the pressure sensors can sense each passing blades. The data in a time window of 0.000375 second were observed for all the radial locations. During this time frame, 5 blades should pass in front of the sensor. Results at different radial location are shown in Figure 4.4. From the plots it is clear that the pressure

transducers were able to identify each passing blade. Five peaks can be observed on each radial location plot. This provided a high confidence in the capability of the transducers to sense very small movements of the blades.
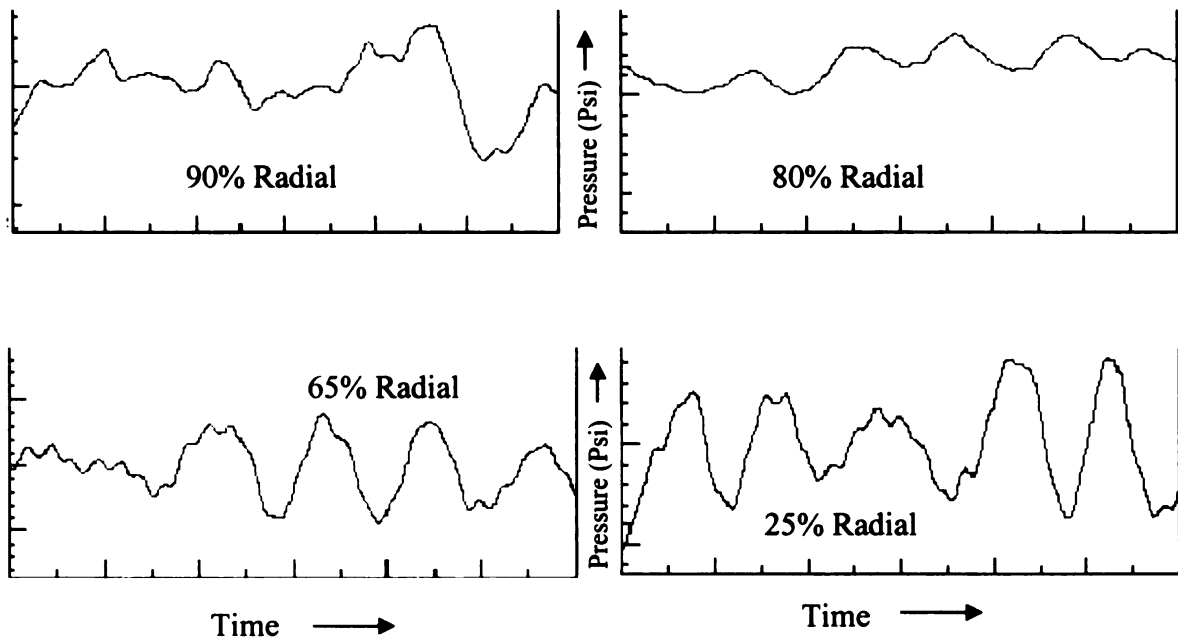


Figure 4.4 Five blades passing observed at various radial locations.

## 4.4   Conclusions

In test 1, the pressure transducers were selected based on the criteria for them to be able to respond accurately in steam environment. The selected transducers were hermetically sealed and were capable of working up to 500°F temperature, which was well above the expected temperature of the steam at last stage blade. During the test, the pressure transducer was able to sense maximum flow at a specific angle. The transducers have the

capability to sense each passing blade individually. The data were reviewed for a very small period of time and the transducers were able to pick each blade passing by the transducer.

# Chapter 5

# Experimental Design and Setup

## 5.1    Hardware Description

The test was performed at General Electric Company's state-of-the-art Low Pressure Development Turbine (LPDT) facility located in Schenectady, New York. LPDT is a subscale low pressure steam turbine that can accommodate up to 4 stages of blades and nozzles. The test rig is designed such that it can operate at various steam turbine operating conditions and can accommodate various blade hardware configurations. To accommodate various blade configurations/sizes, the turbine is designed with two hoods called "hood within a hood". The inner hood is changed to accommodate various steam path designs, while the outer hood remains the same for all test configurations. All the hardware including blades, nozzles and other components of steam path were manufactured by scaling down the full-scale production hardware. Manufacturing tolerances were kept tight to reduce the impact of scaling.

To understand the application of this technique in detail, two separate tests with completely different hardware were performed. The results from both tests are presented in this dissertation. Figures 5.1 and 5.2 show the subscale blades assembled on the rotor

in the lower half of steam turbine inner casing from test 2. The figure 5.3 shows the view of the buttoned-up turbine after assembly.

Pressure and temperature measurements were taken at several key locations in the steam flow path throughout the test facility. In order to understand the flow distribution and performance of the turbine, additional pressure probes were mounted at numerous radial locations in the steam path. In addition to these fixed pressure measurements, five traverses were available in the vicinity of last two blade stages. These traverses can move in radial directions and can rotate 350° to capture the flow field completely.



Figure 5.1 Assembled rotor

Turbine output is measured by two methods: via in line Torque Tronics torque meter and via Kahn water breaks. The torque meter and water breaks are installed directly at the both ends of the rotor. The amount of steam available in summer is around 150,000 lbm/hr ( $6.8 \times 10^4$ kg/hr) and in winter the amount drops to 100,000 lbm/hr

$( 4.5 \times 10^4 \text{kg/hr})$. Steam at maximum pressure of 400 psi (2758 kPa) and temperature of 700°F (371°C) is available and can be adjusted to any desirable test conditions.
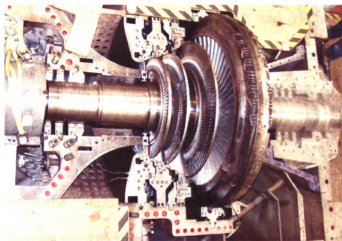


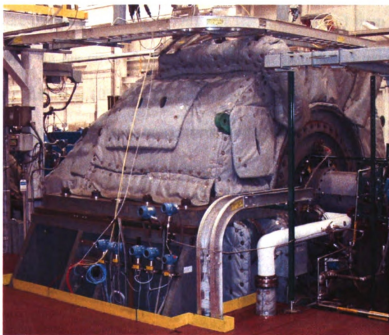Figure 5.2 Assembled rotor in the lower half of steam turbine casing.



Figure 5.3 Assembled subscale turbine during test.

## 5.2 Dynamic Pressure Transducer Locations

As mentioned before, last stage blades are impacted mostly by the aerodynamics instabilities. To capture the vibration response, the dynamic pressure sensors were placed downstream of the last stage blade on the steam guide and on the traverse. In field applications, due to efficiency reasons, it is not possible to have transducers in the steam flow field. But in the test turbine the transducers were placed in the flow field to understand the flow and parameters that cause flutter.

The final goal is to use the transducers in the inner casing close to the covers of the blades. It was expected that the data from the transducers located in the flow field capture clear vibration information. The data from the transducers in the flow field is used to develop a relationship between the data from the transducers located in the flow field to that of the transducers located in the casing. The pressure transducers located on the steam guide were placed at 1 inch (2.5 cm) and 1.5 inch (3.8 cm) from the end of last stage blade covers. In the circumferential direction, the transducers were placed in the upper half of the turbine at 10° from the horizontal joint on each side. Figure 5.4 shows the schematic of dynamic pressure transducers locations in the vicinity of the last stage blade. Figure 5.5 shows the pressure transducers located on the traverse.
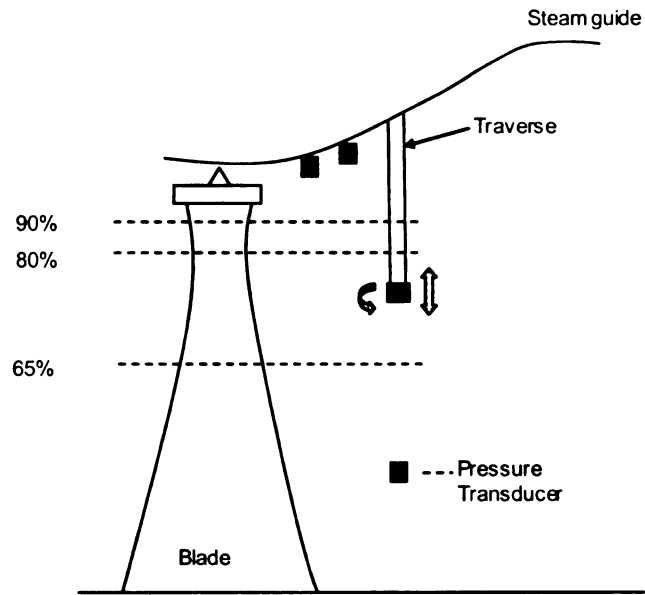
Figure 5.4 Location of pressure transducers in the vicinity of the last stage blade.
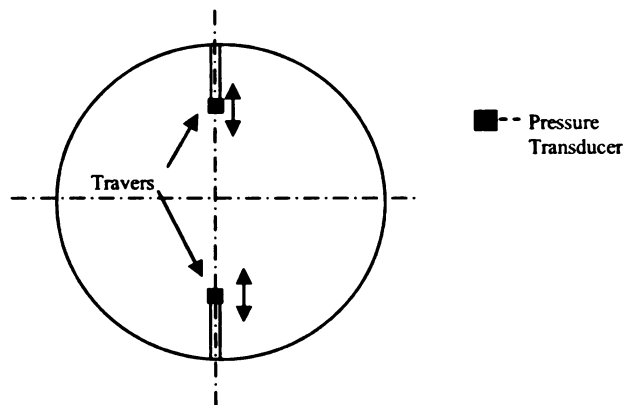


Figure 5.5 Location of pressure transducers on the traverses down stream of last stage

blade.

The test consisted of two main phases. In the first phase, the traverse was moved to various radial locations. At each radial location the transducers were rotated approximately 350° to capture the flow field characteristics. With the traverse rotation, an optimal angle was obtained where the transducer senses highest flow or the flow vector is aligned with the transducer receiving axis. The traverse test was conducted at fixed turbine speed. In the second phase of the test, turbine speed was varied. The traverse was stationary at a radial location and the transducers rotation angle was set to the optimum value obtained from the first phase of the test. Generally this radial location for the traverse was kept close to the tip of the blade.

## 5.3    Strain Gauge Locations

The strain gauges have been used with high level of confidence to predict the natural frequencies and amplitude of the rotating blades. For this reason, the response from dynamic pressure transducers is compared with strain gauge response to validate the accuracy of the dynamic pressure transducer.

In both tests, the strain gauges were placed on the blade vane on the pressure and suction sides at various radial locations. Strain gauges were placed at 5 different locations. At high rotating speeds, the strain gauges experience enormous centrifugal loading and tend to come off from the blade surface. In order to guarantee gauge bonding on the blade surface, the strain gauges were buried under a layer of epoxy and then cured in an oven under pressure. Thermocouples were also mounted on the blade surfaces to monitor

blade temperature. Figure 5.6 shows the strain gauges and thermocouples located on the last stage blade.
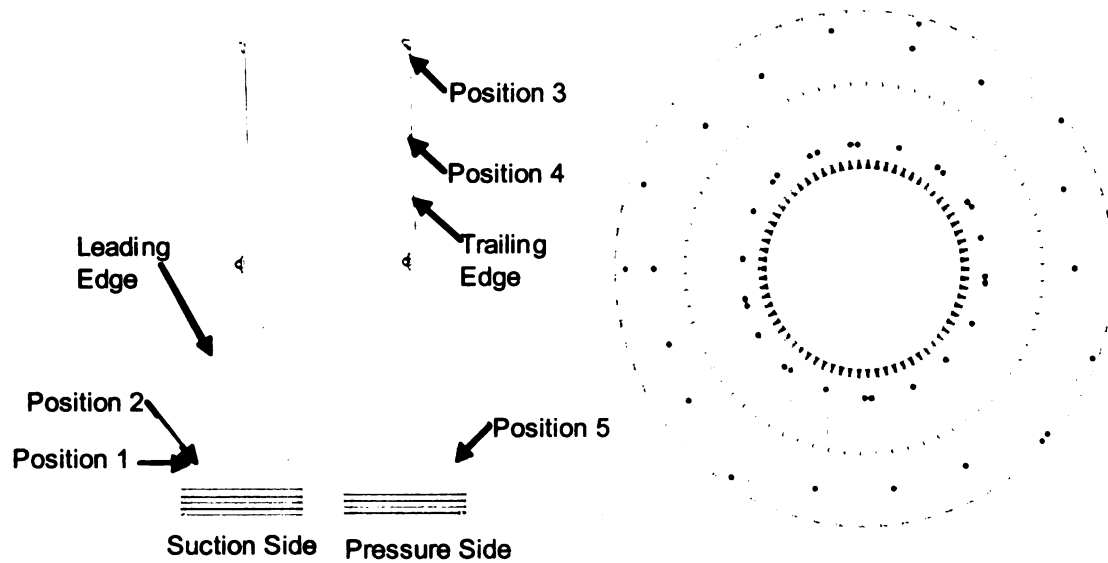


Figure 5.6 Location of strain gauges at the last stage blade

## 5.4 Scaling

The operating conditions were scaled accordingly to the subscale hardware. All the parameters of the turbine operation do not get scaled such as steam moisture droplet size, steam flow velocity, dynamic pressure amplitudes etc. It is assumed that the impact of these factors is negligible. In the published literature, a very limited amount of information is available on scaling effect on steam turbines. From aircraft engines, Jutras et. al. [12] described that a scaled down version of Fan C (at lower Reynolds number) gave the same result in terms of performance and flutter as the full scale version, demonstrating the Reynolds number insensitivity experimentally.

As mentioned earlier, the test was conducted on two different set of blades, both of which were scaled to fit in the subscale turbine space. In both cases, the full scale hardware was tested for frequency response in a vacuum chamber. The blades were excited using air jets and the speed of rotation was changed from 20% to 120% of the operating speed of the blades.

For test 2 hardware, vibration tests were performed on the 50Hz and 60 Hz applications of these blades. A very good agreement is observed in frequency response and a maximum difference of 20Hz is seen for higher order modes. For lower order modes, the difference in frequency is within few Hz. Table 5.1 summarizes the results from the two scaled blades. This proves the concept of scaling of frequencies between two scaled set of blades. Manufacturing variations can impact the scaling and this impact becomes greater when the scale factor is large. The small difference observed between the two scales of blades can be attributed to manufacturing variations.

Other factors that are impacted by scaling include turbine speed. For small scale blades, the turbine operating speed increases with scale factor. The stresses in the blade remain same in various scales as the centrifugal forces and blade areas scale proportionally. For operating conditions, the mass flow rate is scaled and exhaust pressure is not scaled. Few things that do not scale with scale factors are moisture droplet size, velocity and Mach number. Table 5.2 summarizes the impact of scaling on various turbine parameters.

| Per Rev Modes | Size = 1.2 Frequnecy (Hz) | Size= 1 Frequnecy (Hz) | Difference Between Frequency Considering Scaling |
|---|---|---|---|
| 2 | 113 | 134 | 1 |
| | | | |
| 5 | 237 | 282 | 2 |
| 6 | 197 | 228 | 8 |
| | | | |
| 7 | 328 | 387 | 5 |
| 8 | 323 | 364 | 20 |
| 9 | 303 | 349 | 12 |

Table 5.1 Test results of two different scale blades

| Parameter | Original | Down in Scale (*S.F* Scale factor) |
|---|---|---|
| Rotor Speed | $N$ | $N \times S.F.$ |
| Mass Flow | $m$ | $m \times S.F.^2$ |
| Blade Frequency | $F$ | $F \times S.F.$ |
| Power Output | $P$ | $P/_{S.F.}$ |
| Exhaust Steam Velocity | $V_{an}$ | $V_{an}$ |
| Mach Number | $M$ | $M$ |
| Blade Tip Speed | $u$ | $u$ |
| Blade Chord | $C$ | $C/_{S.F.}$ |
| Blade Span | $S$ | $S/_{S.F.}$ |
| Blade Thickness | $T$ | $T/_{S.F.}$ |

Table 5.2 Impact of scaling on frequencies.

## 5.5    Test Points

As mentioned earlier, for steam turbine, the two parameters that have strong influence on the onset of aerodynamics instabilities are the exhaust-pressure and mass flow rate. During the test, both these parameters were varied to study blade response. The test space was a three-dimensional space, with steam mass flow, exhaust-pressure and turbine speed being three variables. Each test point represents a unique combination of two variables that determine the operating condition: exhaust-pressure and steam mass flow. At each test point, the turbine speed is swept through 85% to 115% of the maximum continuous speed.

The test points were selected such that there are more chances of excitation of aerodynamic instabilities. Figure 2.7, in section 2.6, shows strain gauge response of blades on "$V_{an}$ vs. exhaust-pressure" plot. From the plot it is obvious that high responses are observed at low exhaust velocity and high exhaust- pressure. For this test, the test points were mostly in the area where high blade response was observed. Figure5.7 shows the test points on "$V_{an}$ vs. exhaust-pressure" plot.

Test space was defined with operating conditions well beyond the application space of the blade and covers extreme blade operating conditions. The exhaust-pressure was varied between 7 kPa to 54 kPa (~ 2 to 16 in Hg); whereas the steam mass flow rate was varied between 7.1 kg/sec to 26.5 kg/sec.
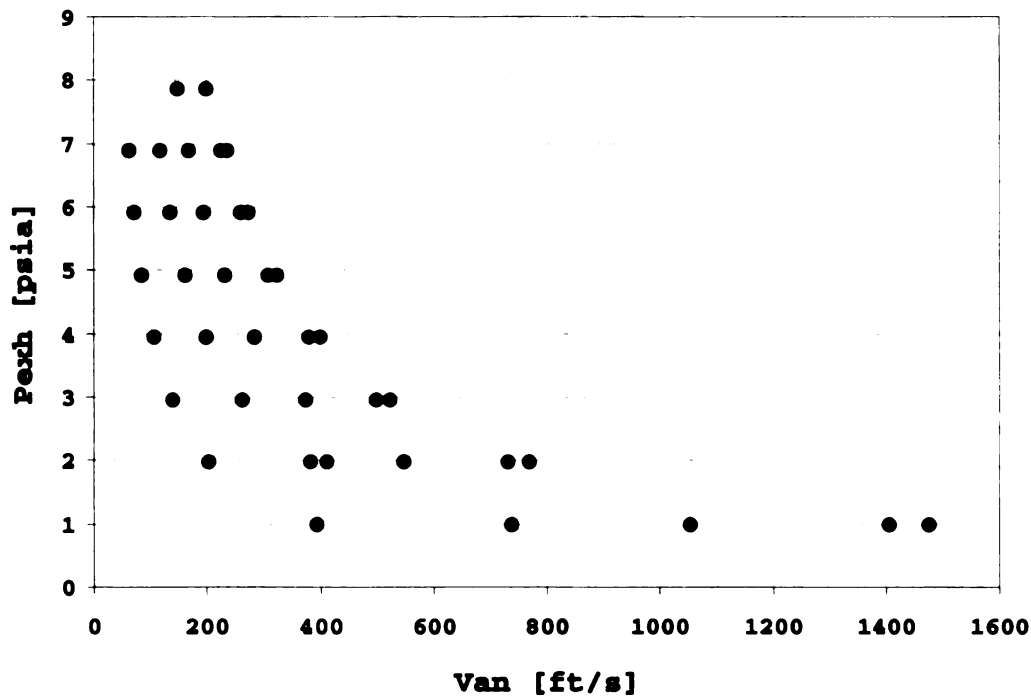
Figure 5.7 Test points shown on "$V_{an}$ vs. exhaust-pressure" plot

## 5.6 Data Acquisition and Evaluation

Data from each measurement instrument was captured and recorded using a data acquisition system developed and installed by Sverdrup Technologies. The data can be viewed real time and exported in ASCII format for later analysis in a spreadsheet or statistical program. Each signal captured from any instrument was ultimately passed through TestView for display, analysis and storage.

The time-dependent signal from the dynamic pressure sensors is transmitted as an analog signal. After analog-to-digital conversion, the signal is sent to a spectrum analyzer for conversion to a frequency-based signal. Fast Fourier transform (FFT) algorithm is used to

convert the signal from time domain to frequency domain. TestLab from LMS is used for data post processing. Analog test data is also stored on data tapes and can be filtered and re-analyzed at a later stage for future investigation of the data. An example of data in time and frequency domain is shown in Figure 5.8.
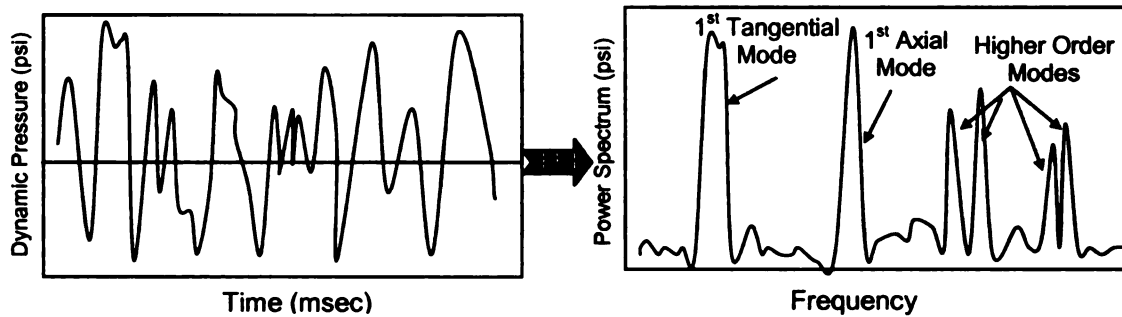


Figure 5.8 Dynamic pressure signals in time and frequency domains.

# CHAPTER 6

# ANALYTICAL PREDICTIONS

With the latest developments in the analytical tools, the accuracy of analysis results has increased significantly. Finite element (FE) analysis tools are used very commonly to predict stresses and frequency response of mechanical systems. With the availability of abundant computer resources, complicated problems are conveniently solved using these commercial analytical tools. FE techniques are used with confidence to predict modal and structural response of assembled row of blades. The key aspect in getting the correct results is the use of appropriate boundary conditions. Stress analysis is generally easier to perform as compared to the frequency response for an assembled row of blades. Different boundary conditions at the connection points between blades at the cover and at the mid span connection can result in different frequency response. In such case the actual hardware is built and tested and then the boundary conditions are adjusted for some modes to match the test results.

## 6.1    Analytical Frequency Predictions

Natural frequencies of a row of blades were predicted using modal cyclic symmetry techniques. One blade with the corresponding wheel/ rotor segment was modeled to predict the natural frequencies of an assembled row of blades. During the first pass in

analysis, various boundary conditions at the cover and at the mid span connection are used. These boundary conditions range from a very loose connection to tighter connection. This helps bound the problem and a range of expected responses is obtained. If test data is available, more precise boundary conditions can be achieved by comparing the two sets of data.

During the modal analysis, cyclic boundary conditions are applied at symmetry planes of the blade and rotor segment. The analysis is done in two steps: in the first step, rotational velocity load is applied and the blade model is allowed to untwist and achieve stiffness of a blade in spinning condition. In the second step, the updated geometry from the first step is used to perform the modal analysis. This step of the analysis provides the mode shapes and resonance frequencies for the assembled row of blades.

A Campbell diagram is then generated to find the crossing of various modes with the engine order lines. For this study, the purpose of calculating the natural frequencies is to have a list of resonance frequencies to understand and distinguish between synchronous and non-synchronous vibrations. As mentioned before, the non-synchronous vibrations are excited by aerodynamics instabilities only.

The frequency analysis was performed for two sets of blades because the test was performed on two sets of hardware. Figure 6.1 shows few mode shapes of the full-scale blade from test 1. Figure 6.2 shows the Campbell diagram for the subscale row of blades from test 1.
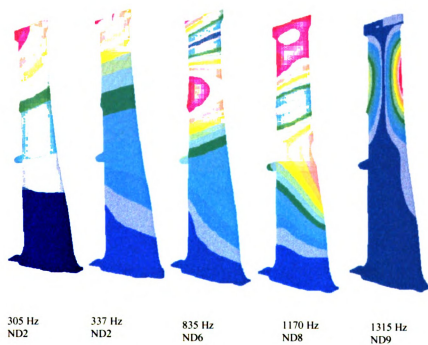
| 305 Hz<br>ND2 | 337 Hz<br>ND2 | 835 Hz<br>ND6 | 1170 Hz<br>ND8 | 1315 Hz<br>ND9 |

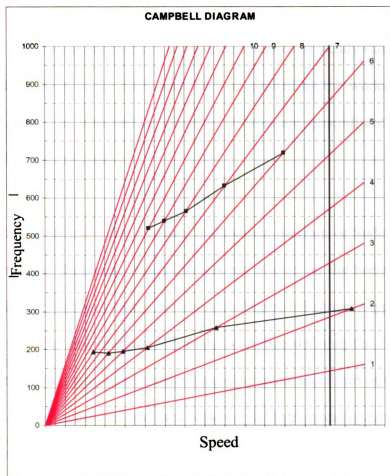Figure 6.1 Mode shapes for the blades

Figure 6.2 Campbell diagram for the subscale blades

## 6.2    Allowable Strain Limits

Before conducting the test, maximum strain levels at various locations on the blades were predicted.    Strain gauges were placed at location, where higher responses during resonance conditions are expected. Mean stresses from static analysis and vibratory stresses from the modal analysis are used to define the allowable strain limits. During the test, strain gauge response was monitored in real time to guard against any unexpected high amplitude vibrations.

## Strain Limits:

Rotating blades in the steam turbine are exposed to a variety of steady state and transient stresses. Centrifugal load of the blade and the load applied by the working fluid cause steady state stresses. The transient or vibratory stresses are generally attributed to the loading caused by blade resonance.

To define a criterion for allowable stresses, a Goodman diagram or Soderberg Diagram can be used. On these diagrams, steady stresses are plotted on the horizontal axis and alternating or vibratory stresses on the vertical axis. Figure 6.3 shows a typical Goodman diagram with the nodal stresses from FE analysis. A line defining the failure limits is obtained by joining yield stress on horizontal axis and endurance limit of the material on the vertical axis. If the failure line is drawn between yield stress and endurance limit, it is called a Soderberg Diagram, whereas in Goodman Diagram, the failure line is drawn between Ultimate strength and endurance limit. This diagram is obtained by performing a series of tests on the material specimens. To ensure a robust design, the failure line is reduced by applying safety factors. Bloch [15] presented formula to calculate factor of safety as

$$\frac{1}{F.S.} = \frac{\sigma_{SS}}{YieldStrength} + \frac{\sigma_{vib}}{EnduranceLimit}$$

Additional safety factors due to manufacturing variation and measurement uncertainties are added to the original safety factor. Some manufacturer also use experience based safety factors.
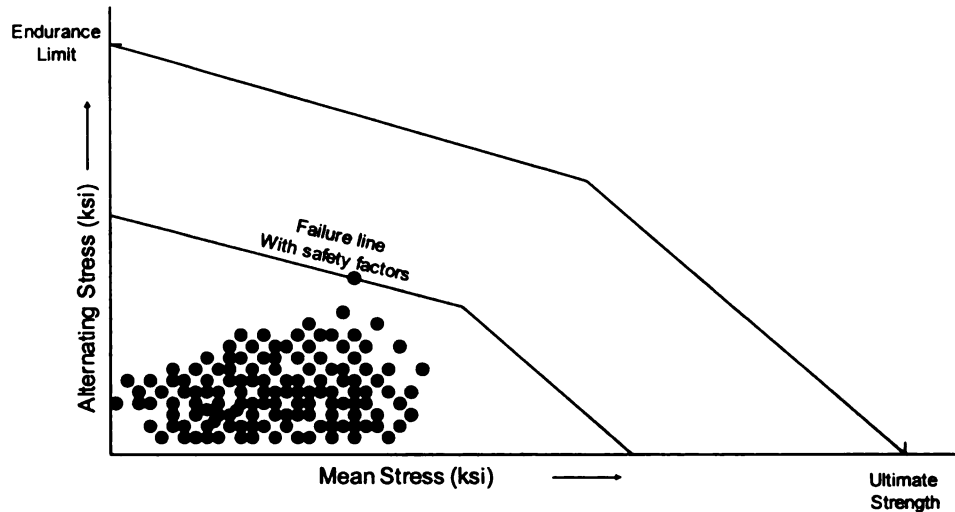
Fig. 6.3 Goodman diagram with the nodal stresses from the FE analysis.

Allowable strain limits are obtained using the Goodman diagram. Steady state finite element analysis of the blades provides the means stresses, whereas the normalized alternating stresses are obtained from the cyclic symmetry analysis. Strain limits for each vibration mode is obtained by plotting the nodal stresses on the Goodman diagram with maximum nodal stress touching the failure line. This provides the maximum allowable alternating stress at various locations on the blade for one mode. This procedure is repeated for all the modes of interest and desired nodal diameters. A matrix of allowable alternating stresses for all the modes is generated. From this matrix, maximum stresses and strains at locations of interest on the blade are identified for every mode. In figures 6.3, 6.4 and 6.5, the dots under the failure line show the stresses at various nodes in the FE analysis. During the test, each strain gauge was monitored real time not to exceed these allowable strains.
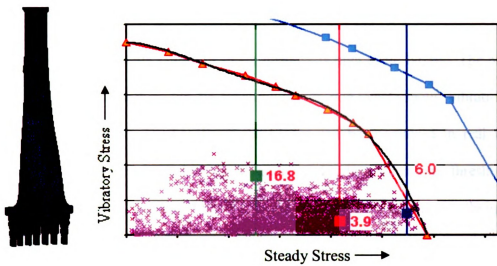
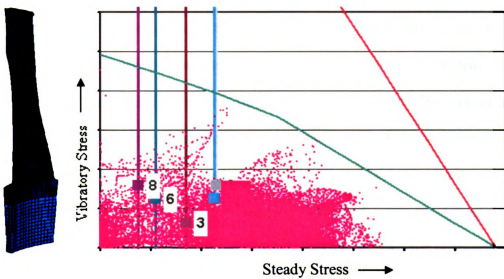Figure 6.4 Nodal response from Test 1 is plotted on a Goodman diagram.



Figure 6.5 Nodal response from Test 2 is plotted on a Goodman diagram.

## 6.3    Allowable Dynamic Pressure Limits

The leading cause of blade failure in steam turbines is high cycle fatigue. The blades are exposed to this risk either due to synchronous or non-synchronous vibrations. This danger can be reduced significantly if the blades can be monitored in real time and necessary measures are taken when the vibration amplitude reaches some threshold value. Chapter 3 has listed various existing blade vibration monitoring techniques and limitations associated with them.

As mentioned earlier, the dynamic pressure transducers were placed at the perimeter of the last stage blade towards the downstream end. When the blades start vibrating, the energy from the blade is transmitted to the steam around it. This transfer of energy to the steam is at the same frequency as that of blade. When this steam reaches the nearby pressure transducer, the pressure transducer senses the harmonic content in steam. Amplitudes of the dynamic pressure depend on the location of the transducers with respect to the blade and upon amplitude of the vibration itself. To guard against the blade failure due to high vibration amplitudes, allowable dynamic pressure limits are required as a function of the distance from the transducer. During the test, the dynamic pressure amplitudes were not used to guard against blade failure. In the final application of this technique, the dynamic pressure amplitudes are used to define Alarm and Trip limits for the turbine.

To obtain the allowable pressure limits, pressure amplitudes and corresponding strain amplitudes measured in the test are compared for various modes. For a location of dynamic pressure transducer, a correlation can be made between the strain amplitude and the pressure amplitude. For example, at a resonance condition the strain gauge response is 50 microstrain and the corresponding dynamic pressure amplitude change measured by pressure transducer is 0.2 psi, which implies that pressure amplitude is 0.2/50 times the strain gauge amplitude. If for this resonance condition, the allowable strain limit based on the Goodman diagram is 200 microstrain, then the allowable pressure limit for the pressure transducers is 200*0.2/50 or 0.8 psi. The pressure limits obtained using this approach is based on the material capability of the blade. The safety factors that were used to get the failure limits on the Goodman diagram are included in these limits. An Alarm and Trip can be defined for the turbine based on the responses observed at various turbine operating conditions.

An extension to this work can be done by defining alarm and trip limits for the turbine based upon specific frequency ranges. This will provide even greater operational flexibility to the turbine

## 6.4 CFD Analysis

CFD analysis was performed to understand the impact of change of exhaust-pressure on the flow at the last stage blade. Two-dimensional CFD analysis is performed. Mass flow and inlet conditions were kept constant. The exhaust exhaust-pressure is varied during the

analysis from 1 in HgA to 6 in HgA. The results have shown that with increasing exhaust-pressure, the flow separation starts at the hub. As the exhaust-pressure increases from the design point, the flow tends to migrate towards the tip section and separation zone increases. Figure 6.6 shows the result of the analysis. The last stage blade boundaries are show with red color lines.
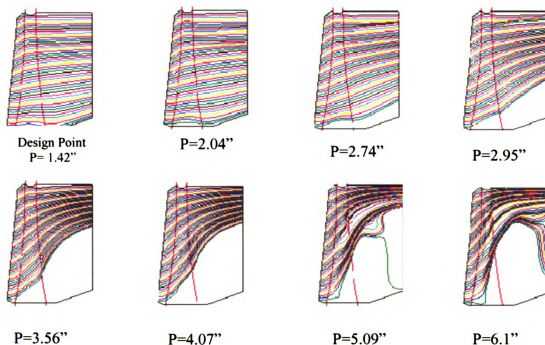


Figure 6.6  Flow reversal at the hub as a function of condenser exhaust-pressure.

## 6.4    Conclusions

Details of structural, modal response prediction are presented and the challenges associated with that are discussed. Following conclusions can be made from the analysis

- Accurate frequencies can be predicted for the assembled row of blades.

- Boundary conditions for the modal analysis can be calibrated based on the full scale hardware test.

- The limits for the strain were determined using the mean and alternating stresses obtained for static and modal analysis. Material Goodman diagrams with adequate safety margins were used for the strain limits.

- Allowable dynamic pressure limits based on the strain limits are calculated. Allowable pressure limits can be applied with confidence as these are based upon the Goodman diagram with safety margins built into them.

- CFD analysis shows that at higher exhaust-pressure, flow separation starts at the blade hub. This separation zone increases with increasing exhaust-pressure.

# CHAPTER 7

# EXPERIMENTAL RESULTS AND

# COMPARISON

There were two tests conducted to validate the proposed technique. The purpose of Test 1 was to select appropriate pressure transducers that can operate satisfactorily in the steam environment. In test 2, the selected transducers were used at wide range of turbine operating conditions by changing steam mass flow, exhaust pressure and turbine speed. The test consisted of two phases. In the first phase, the pressure sensor located on the traverse was moved to four different radial locations and at each location the sensor was rotated by 350°. During this phase an optimal location and rotation angle of the pressure transducer was obtained. In the second phase of the test, the transducer on the traverse was fixed at the optimal orientation identified in the first phase. The turbine speed was varied from 85% to 115% of the maximum continuous speed. Data were recorded during ramp up and ramp down of speed.

## 7.1   Test Results

The results presented in this section cover phase 1 of both tests. In the relevant sections, the results from both tests are described and compared. The impact of change in dynamic pressure response due to mass flow and exhaust pressure is studied. Riaz et. al. [22] has summarized the results of this work.

### 7.1.1   Flow Angle Detection

Orientation of the dynamic pressure transducer is critical for capturing the flow characteristics. At any test points, maximum flow amplitude is observed at a certain angle. At this angle the flow direction and transducer receiving axis are aligned. This is a function of the exit angle of vane trailing edge. As the sensor is not in close proximity of the blade, due to turbulence in flow field, this angle was not consistent and was within 5% of the nominal value. In most of the test points, at ~ 132°, the transducer was facing the flow field. Figure 7.1 shows the response from the pressure transducer at 80% radial location of the blade. This angle measured for test 1 was around 135°.
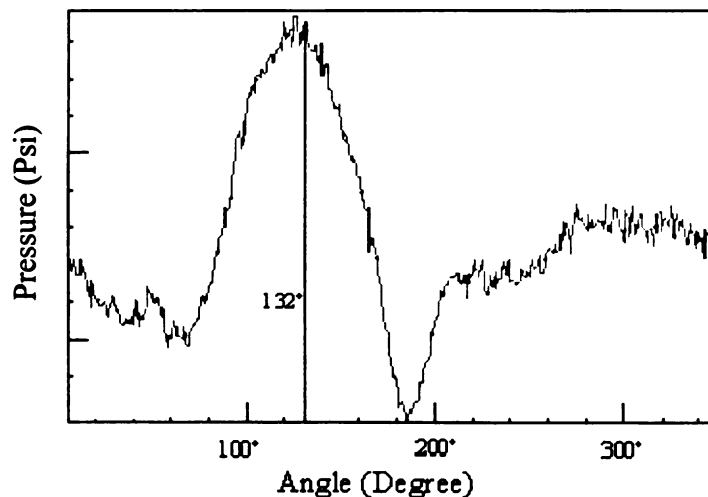
Figure 7.1 Dynamic pressure amplitude verses traverse rotation angle.

76

In the second phase of the test, an angle of 132° is kept for the traverse pressure transducer while speed was varied between 85% and 115% of the operating speed. In the speed sweep, the data were recorded from strain gauges and pressure transducers located on the steam guide and traverse.

## 7.1.2 Flow Separation Phenomenon

CFD analysis has shown that at higher exhaust-pressure, the steam tends to move towards the tip of the blade. To confirm this phenomenon, the pressure transducers located on the traverse was moved to various radial locations of the blade. During test 1, the traverse data were taken at 4 radial locations at 25%, 65%, 80% and 90% radial height of the blade with 0% being at the hub and 100% at the tip of the blade. At each radial location the traverse was rotated to find the location of maximum response. At each radial location, maximum response is plotted in Figure 7.2. The plot clearly shows that the maximum pressure amplitude is observed at 90% radial location and very small dynamic pressure change is observed at and below 65% radial height of the blade.

Based on the experience from test 1, all the data collected in test 2 were above 65% radial height of the blade. With increasing exhaust-pressure, similar hub separation phenomenon was observed. In test 2, the impact of steam mass flow variation on the flow separation was also studied. With a low flow condition, the transducers picked weak pressure response. With increasing mass flow, higher responses were observed at the transducers.
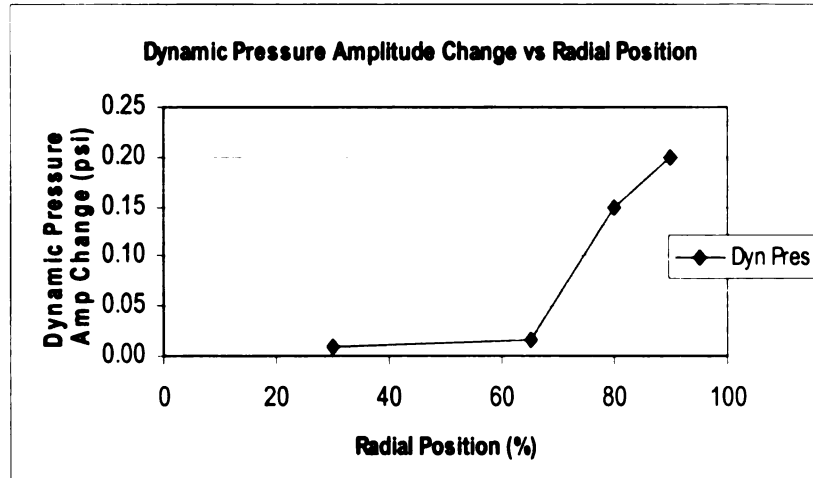
77

Figure 7.2 Dynamic pressure amplitudes at various blade radial heights.

Flow separation at the blade hub was more prominent with increasing exhaust pressure. This is due to the fact that at higher exhaust-pressure, the higher-pressure steam in the exhaust leads to a higher density, and thus a lower volumetric flow rate, resulting in the steam migrating towards the tip of the blade. At the same time, when the turbine is spinning, the heavy steam (with moisture content) tends to move towards the outer periphery of the steam flow path. Figure 7.3 shows the dynamic pressure amplitude at three different flow conditions, maximum flow is observed close to the tip. Results from both test validates CFD analysis and prove that the dynamic pressure transducers can successfully capture change in pressure variation with changing flow conditions.
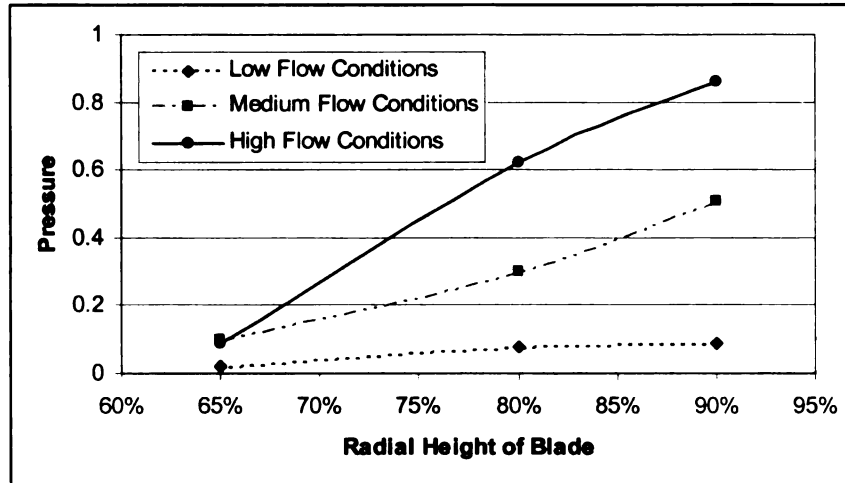
Figure 7.3 Dynamic pressure amplitude verses blade height

## 7.2 Comparison of Strain Gauge and Pressure Transducers Results

Strain gauge data were recorded throughout the test along with dynamic pressure transducers data. A comparison between two sets of data shows a very good agreement. From the results of test 1, two modes at 300Hz and 800Hz were observed by strain gauges. Dynamic pressure transducers were also clearly able to identify these two frequencies. Figure 7.4 shows the spectrum plot from dynamic pressure transducers with two frequencies identified. Figure 7.5 shows the response from strain gauges with same frequencies. FE analysis also predicted these two frequencies. Campbell diagram for the subscale blades in Figure 6.3 shows the crossings of first and second mode with engine-order lines at these frequencies. This proves the validity of predictions by the FE analysis.

In test 2, similar relationship between the two sets of data was observed. Figure 7.6 shows a comparison between two responses from the strain gauge and pressure

79

transducers. Pressure transducers were clearly able to pick up frequencies that were observed by the strain gauges. 300, 400 and 800Hz modes are clearly visible in both plots. These modes were prominent and were observed in most of the test points. FE analysis also predicted similar results. It can be concluded that, from two different tests, the dynamic pressure transducers were clearly able to sense the frequencies that were observed by the strain gauges.
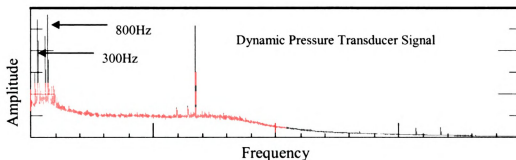


Figure 7.4 Dynamic pressure sensors show a clear response at 300 and 800Hz frequency.
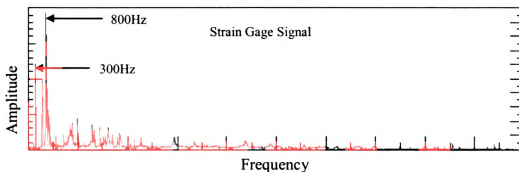


Figure 7.5 Signal from strain gauges shows a clear response at 300 and 800Hz frequency.
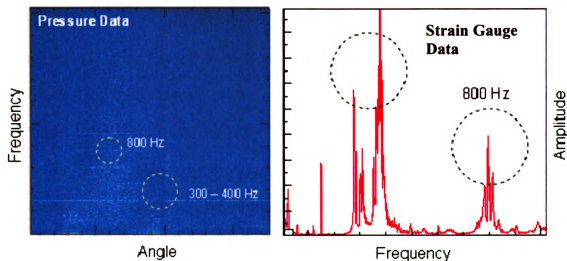
Figure 7.6 Comparison between pressure sensor and strain gauge data.

## 7.3 Engine Order Modes Tracking

Assembled row of blades are exposed to synchronous or non synchronous vibrations. Synchronous vibrations occur, when a mode of vibration crosses one of the per-rev or engine order line. For a turbine speed sweep, a response can be observed for a per-rev excitation if one of the modes crosses that per-rev line. For better understanding of the dynamic pressure transducers application, the per-rev responses were divided into lower per-rev (order) and higher per-rev (order) responses. For higher order responses, the bandwidth for data acquisition was kept at 40 kHz and for lower order responses it was 2 kHz.

## 7.3.1 Higher Order Modes Tracking

The main objective of using pressure transducers in the turbine is to pick up various vibration modes of the rotating blades. One of the expected higher order mode was the blade passing frequency mode. If "F" is the number of blades in a row, the pressure transducers were clearly able to pick up the 1F, 2F and 3F order blade passing frequencies. Another interesting observation was that the pressure transducers also sensed the 1F frequency from the one stage before the last stage blades. This means that the harmonic content in the steam from one stage remains in the steam even after passing through the following stage. The transducer was found to be sensitive enough to capture this weak response. Figures 7.7 shows the Campbell diagram with blade passing frequencies during speed ramp up from the pressure transducer located on the traverse.

The transducers located on the steam guide also responded accurately and were able to pick up the blade passing frequencies. Figure 7.8 shows the response observed by pressure transducers located on the steam guide. Both the stationary transducers were able to pick up the 3 blade passing frequencies, which were observed by the transducers located on traverse at 90% radial height location in the steam field. The higher order modes generally have less energy and are difficult to observe, but the transducers were able to identify them. Therefore it can be concluded that the pressure transducers located on the steam guide were accurate enough to sense these higher order modes.
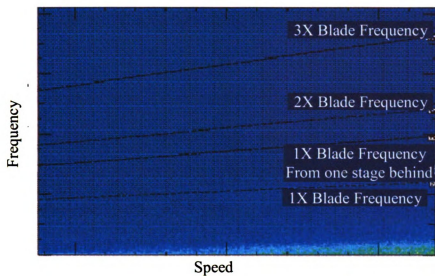
Figure 7.7 Campbell diagram showing blade passing frequencies observed with pressure
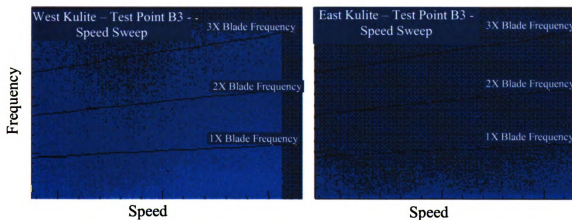
transducers located at traverse.



Figure 7.8 Campbell diagram showing blade passing frequencies picked at sensors

located at steam guide

## 7.3.2 Lower Order Modes Tracking

In order to track lower order modes, the frequency bandwidth was set low. With higher bandwidths, the lower per rev modes data get corrupted due to windowing function used in data acquisition. In the test points with lower frequency bandwidths, the pressure transducers were successfully able to pick up lower order modes. Figure 7.9 shows the Campbell diagram with 2/rev, 3/rev and 7/rev responses observed using a pressure transducer on the traverse.

Pressure amplitudes are compared from traverse and stationary transducers and a correlation can easily be found. For the field application, this correlation is necessary because it is not desirable to have pressure transducers in the flow field.
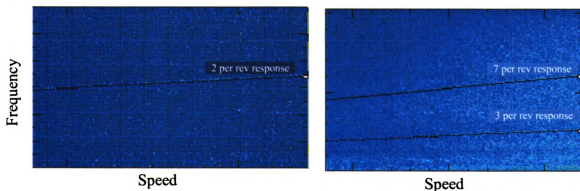


Figure 7.9 Campbell diagram showing 2, 3 & 7 per rev modes.

These results were compared with strain gauge results to verify similar responses. The 2 per rev mode, which is a higher energy mode, is clearly visible on strain gauges and

pressure transducer responses on all the test points. 7/rev response was also observed on strain gauges and is clearly seen on the pressure transducers as shown in Figure 7.9.

## 7.5 Conclusions

The results are highly encouraging and show significant achievement towards the success of this technique. The pressure transducers can be used to monitor real time vibration behavior of the blades. Following conclusions can be made from the tests performed:

- Dynamic pressure transducers were used in two different tests with different hardware and operating conditions and similar results were observed proving the reliability of this technique.

- Consistent flow angles were observed in different test points.

- The pressure transducers with increasing exhaust-pressure captured flow separation at the hub of the blade. CFD analysis was validated.

- Higher responses at the pressure transducers were observed with increasing mass flow.

- Blade vibration frequencies observed by dynamic pressure transducers match the strain gauge frequencies. These responses also match with the FE analysis prediction.

- The pressure transducers located on the steam guide and at the traverse observed higher order modes such as blade passing frequencies.

- The pressure transducers also sensed blade passing frequency from the one stage before the last stage blades. This implies that the harmonic content in the steam

from one stage remains in the steam even after passing through the following stage.

- Lower order modes such as 2, 3 and 7 per-rev were clearly observed by the dynamic pressure transducers and strain gauges.

In summary, the pressure transducers were able to detect weak as well as strong responses that were observed by strain gauges. Therefore, it can be used as an alternate method for real time blade vibration monitoring with high level of confidence. This technique is easy to implement on in-service steam turbines as compared to existing techniques such as use of strain gauges, laser Doppler vibrometry, frequency modulated grid system etc. The pressure transducers can easily be installed/ replaced without removing the upper hood of the turbine or removing the rotor, which is required in other techniques. Properly designed tubes with transducers can be inserted from the outer hood of the machine in the holes located close to the last stage blade cover. Overall results and ease of application proves that pressure transducers can be easily used as an alternative method to monitor the blade vibrations.

# CHAPTER 8

# CONCLUSIONS AND RECOMMENDATIONS

The successful operation of a steam turbine depends largely on the structural integrity of its rotating components. The magnitude of vibratory and static stresses defines the structural integrity of these components. Vibrations induced by aerodynamic instabilities have always been a concern for blade designers. Exhaust-pressure at the condenser has been identified as the main source of aerodynamics instabilities and a critical factor that limits the operating range of steam turbines.

Dynamic pressure transducers have been proved as an alternate experimental technique for detection of any type of vibrations in steam turbines. Test results have shown that this technique can be used successfully for blade vibration monitoring. The onset of any vibration can be detected, thereby providing protection to the blades from aerodynamic instabilities. With proper orientation of the pressure transducers, prominent vibration modes were detected accurately. The real time blade monitoring allows the turbine to operate at higher exhaust-pressures without any concern of failure due to HCF.

Allowable pressure limits for the use of dynamic pressure transducers are identified based on the material capability of the blade. Material Goodman diagram with adequate safety

factors were used to define the allowable pressure limits. Therefore the blades can operate to their maximum capability. For selection of dynamic pressure transducers, moisture level on the last stage blade can lead to transducer inaccuracies, so proper sealing of pressure transducers is mandatory.

Since the test was performed on a subscale turbine, frequency scaling issues were addressed by performing vibration tests on two different scales of a blade. The test was conducted in vacuum chamber and the blades were excited with air jet. The results showed excellent agreement between two set of frequencies.

As a next step towards implementing this technique in the production turbines, a full scale turbine test will be required. The pressure levels will be higher in the full scale turbines and may not be scaled. Another extension to this work can be done by defining alarm and trip points based on specific frequency ranges. This will provide even greater operational flexibility to the turbine. Based on the modal frequencies, allowable pressure levels can be defined. An example of such a control schedule can be defined as shown in Table 8.1

| Frequency Range (Hertz) | Alarm Level (psi) | Trip Level (psi) |
|---|---|---|
| 0 – 100 | 0.5 | 1.0 |
| 100 – 1000 | 0.1 | 0.5 |
| 1000 – 5000 | 0.05 | 0.1 |
| > 5000 | 0.01 | 0.05 |

Table 8.1 Allowable pressure amplitudes for different frequency ranges.

Above mentioned values are for reference only. The actual frequency and pressure levels must be defined separately for each blade. Actual pressure levels will also be based on multiple factors such as material properties, resonance characteristics, excitation sources, and effect of damping.

The ease of installing and removing pressure transducers on in-service turbines makes this a very convenient technique. Probes carrying dynamic pressure sensors can be placed /replaced in the turbine without opening upper casing of the turbine.

This technique will not only be able to monitor the vibrating blades but at the same time will provide a safe and reliable steam turbine. They can be operated without any risk at the times when power demands are high. More power can be produced resulting in huge financial gains for power plat owners and will help meet the high energy demands of future.

# Bibliography

[1] Riaz, M. S., Barb, K. J. and Engeda, A., 2005, *A novel technique for steam turbine exhaust-pressure limitation using dynamic pressure sensors,* Journal of Mechanical Engineering Science Proceedings of the Institution of Mechanical Engineers Vol. 219 Part C:

[2] L.E. DRAIN, 1980, The *Laser Doppler Techniques,* Wiley, London, Chapter 9

[3] A. V. SRINIVASAN, 1997, *Flutter and Resonant Vibration Characteristics of Engine Blades.* Transactions of the ASME, 42nd International Gas Turbine and Aeroengine Congress and Exhibition, Orlando, Florida. Vol. 119, pg 742-775

[4] EVANS, D, 1992, *Comparison of unstalled flutter predictions and field measurements for steam turbine blades.* Proceedings of the Steam and Combustion Turbine-blading Conference and Workshop, Pages 4/85-4/99

[5] K.D. WANG, R.S. AMANO, 1998, *Turbulent instability prediction in low pressure last stage steam turbine blades.* Proceedings of the ASME Heat Transfer Division, Vol 361-1, pg 109- 116

[6] LAZAN, B.J. 1968, *Damping of materials and members in structural mechanics.* The fifth edition, Pergamon Press

[7] P.ROZELLE, P.D.HILL, *Time-of-arrival vibration measurements for design verification of rotating turbine blades.* Westinghouse Electric Corporation.

[8] H. W. LIEPMANN, 1952, *On the Application of Statistical Concepts to the Buffeting Problem,* Journal of Aeronautical Sciences, Vol. 19, Number 12, Pg 793- 800

[9] R. D. BLEVINS, 1990, Flow Induced Vibrations, Second Editions, Published by Van Nostrand Reinhold, New York.

[10] S. Pines, 1958, *An elementary explanation of the flutter mechanism.* Proceedings National Specialists meeting on Dynamics and Aeroelasticity, Institute on the Aeronautical Sciences, Ft. Worth. TX

[11] Y. C. Fung, 1969, *An introduction to the Theory of Aeroelasticity*, Dover New York, pp. 194-195

[12] Justras, R. R., Fost, R. B., Chi, R.M., Beacher, B. F., *Subsoinc/ transonic stall flutter investigation of a rotating rig.* Technical report, NASA, 1983. NASA CR-174625

[13] Z. Hu, G. Eyb, D. Regnery, 2002, *Experience with the non-contacting blade vibration measurement methods using two sensors in a low pressure model steam turbine.* Proceedings of IJPGC'02, 2002 International Joint Power Generation Conference, pp 273-281

[14] B. Halkon, 2002, *Turbomachinery Blade Vibration Analysis*, PhD Dissertation, Loughborough University.

[15] Bloch, Heinz P., *A Practical Guide to Steam Turbine Technology*, Mc-Graw Hill Publishing, p. 179-183, 1996.

[16] D.L. Bell, L. He, 2000, *Three Dimensional Unsteady flow for oscillating turbine blade and the influence of tip leakage.* Journal of turbomachinary, Vol 122, Pg 93-101

[17] O.J.R Queune, L. He, 2001, *Experimental study of 3D unsteady flow around oscillating blade with part-span separation.* Journal of Turbomachinary, Vol 123, pp 519-522

[18] L. He, 1998, *Unsteady flow in Oscillating Turbine Cascade: Part1, linear Cascade experiment,* Transactions of the ASME, Vol 120, pp 262-268

[19] F. Truckenmuller, W. Gerschutz, H. Stetter, H. Hosenfeld, 1998, *Examinations at a three stage low pressure model turbine during ventilation.* PWR-vol. 33 International Joint Power generation conference. Volume 2, pp 473-482

[20]W. G. Steltz, 1999, *An approach to resolving the very low flow phenomenon in low pressure steam turbines*. PWR-Vol. 34, 1999 Joint Power Generation Conference, Vol 2, pp 433-439.


[21] J.R. KADAMBI, R.D. QUINN and M.L. ADAMS, 1988, *Non-intrusive turbomachinary blade vibration and stress measurement techniques*. Transaction of the American society of Mechanical Engineers: Power Division (Publication) PWR, #, 197-205.


[22] Riaz, M. S., Barb, K. J. and Engeda, A., 2005, *An Experimental Technique to Monitor Aerodynamic Instabilities in Steam Turbines*, Submitted to Journal of Mechanical Engineering Science, Institution of Mechanical Engineers